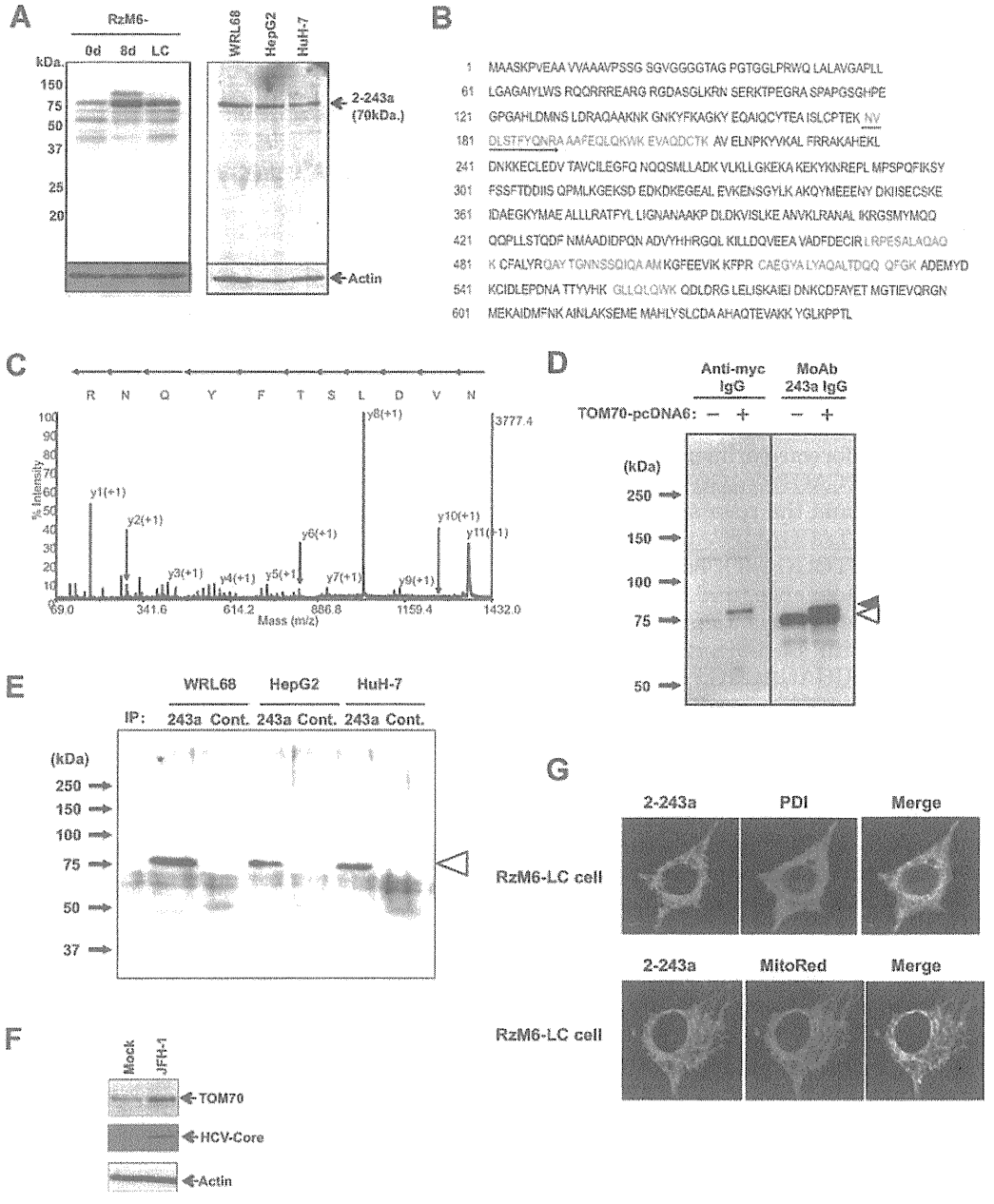

Fig. 1. TOM70 is induced by HCV and is localized in the mitochondria. **A**: TOM70 induction was examined by WB in RzM6-8d and RzM6-LC days (left panel), and TOM70 expression was compared in WRL68, HepG2, and HuH-7 cells (right panel). **B**: Identification of p70 by MALDI-TOF-MS analysis. The sequence of peptides in the amino acid sequence of TOM70 protein was determined using MALDI-TOF-MS analysis (red characters). **C**: MS/MS spectra of the peptide NVDLSTFYQNR (149–159). The sequence covers 14% of the amino acid sequence of TOM70. **D**: Identification of p70 by IP-WB. Expression of TOM70-pcDNA6 in HuH-7. Cell lysates were examined using WB with mAb 2-243a or the anti-myc antibody. myc-TOM70-pcDNA6 expression was recognized by both mAb 2-243a and the anti-myc antibody (black triangle). The expression of cellular TOM70 (empty triangle) was recognized only by mAb 2-243a. **E**: Cell lysates were immunoprecipitated with anti-rat TOM70 antibody and analyzed using WB with mAb 2-243a. The empty triangle indicates TOM70. The molecular weight markers are shown on the left. **F**: Expression of TOM70 and the core protein in mock- and HCV JFH-1-infected HuH-7 cells. **G**: Localization of TOM70 in RzM6-LC cells. The cells were stained with mAb 2-243a and polyclonal antibody against PDI or MitoRed. The magnification is 800×.

antibody (CH-11; 0–20 ng/ml; Beckman Coulter, Murmasaka) or recombinant human TNF-α (0–100 ng/ml; PeproTech, Rocky Hill, NJ), followed by addition of cycloheximide (CHX; 10 μg/ml). After treatment for 24 hr, apoptotic cell death was evaluated by determining cell viability with the WST-8 reagent. Next, the terminal deoxynucleotidyl transferase dUTP nick-end labeling (TUNEL) assay was performed using the TMR red in situ cell death detection kit (Roche, Basel, Switzerland).

Generation of Small Interfering Ribonucleic Acid (siRNA) for TOM70

siRNAs for two regions of TOM70, namely, TOM70-d1-siRNA (primer set: TOM70-dicer1-F and TOM70-dicer1-R) and TOM70-d2-siRNA (primer set: TOM70-dicer2-F and TOM70-dicer2-R) were generated.

Gene-specific dsDNA for TOM70 was constructed by PCR using TOM70-pcDNA6 as the template. TOM70-dicer1-F (5′-GCGTAATACGACTCACTATAGGGAGATGTTTGGCCTTTAAGTATCC-3′) was used as the forward primer, and TOM70-dicer1-R (5′-GCGTAATACGACTCACTATAGGGAGATGATATCATCCGTGAAAGAAC-3′) was used as the reverse primer; both primers contained a T7 promoter sequence (underlined). PCR performed using these primers yielded a 434-bp product. PCR with the forward primer TOM70-dicer2-F (5′-GCGTAATACGACTCACTATAGGGAGAATGTTTGCATTGTACCGCC-3′) and the reverse primer TOM70-dicer2-R2 (5′-GCGTAATACGACTCACTATAGGGAGATTTGCAACTTCTGTCTGGGC-3′), both of which contained a T7 promoter sequence (underlined), yielded a 474-bp product. Luciferase was amplified from pGL3-Basic (Takara Bio) with Luci-dicer2-F (5′-GCGTAATACGACTCACTATAGGGAGACGGTTTTGGAATGTTTACTAC-3′) as the forward primer and Luci-dicer2-R (5′-GCGTAATACGACTCACTATAGGGAGAGCTGATGTAGTCTCAGTGAGC-3′), as the reverse primer, yielding a 309-bp product; both primers contained a T7 promoter sequence (underlined). LA *Taq* polymerase was used for the PCR. All PCR products were analyzed by agarose electrophoresis before purification with the Wizard SV Gel and PCR Clean-Up System (Promega, Madison, WI).

In vitro transcription was performed with the Dicer siRNA generation kit (Genlantis, San Diego, CA), according to the manufacturer's instructions. Briefly, in vitro transcription reactions were performed in a 20-μl volume with 1 μg PCR product as the template; the reaction mixture was incubated at 37°C for 4 hr, followed by purification with the reagents provided in the Dicer siRNA generation kit. The dsDNA (20 μl) obtained was finally in a 100-μl volume after incubation at 37°C for 27 hr. The siRNAs obtained were purified and quantified according to the manufacturer's instructions.

Next, the cells were plated in 24- or 96-well plates (BD Bioscience, Sparks, MD) at a density of 5×10^4 or 10^4 cells/well, respectively, and left overnight for adherence. The siRNAs (14 nM) generated were transfected to cells by using Lipofectamine RNAiMAX (Invitrogen) and Opti-MEM (Invitrogen). The cells were characterized 48 hr after transfection.

Caspase Assay

The activities of caspase-3/7, caspase-8, and caspase-9 were measured on the basis of the cleavage of a proluminescent substrate containing the DEVD sequence, by using the commercially available Caspase-Glo 9 Assay, Caspase-Glo 8 Assay, and Caspase-Glo 3/7 Assay kits (Promega) and a luminometer (Aloka, Tokyo, Japan). Caspase activity was quantified according to the manufacturer's instructions.

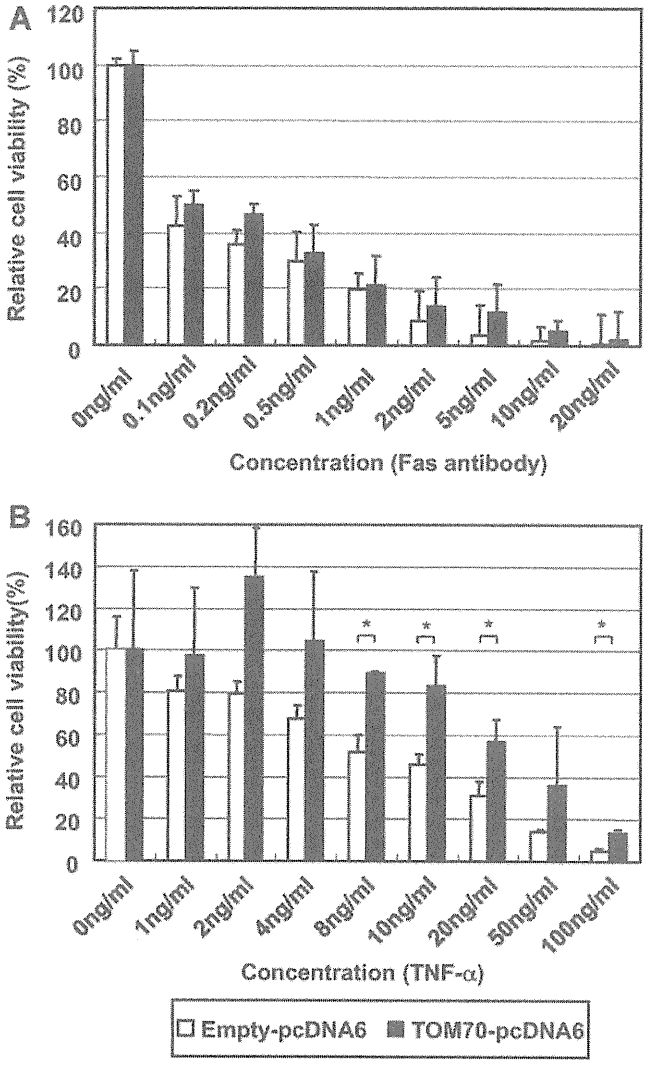

Fig. 2. TOM70 overexpression induced TNF-α-mediated apoptotic resistance. TOM70 overexpression affected TNF-α-mediated apoptosis but not Fas-mediated apoptosis. Cells were transfected with empty pcDNA6 (white bar) or TOM70-pcDNA6 (black bar). After 48 hr, they were treated with (A) Fas antibody (0–20 ng/ml) or (B) TNF-α (0–100 ng/ml). After 24 hr, cell viability was measured using WST-8. A,B: The data represent the average of the values obtained from triplicate experiments, and the vertical bars indicate the SD. $^*P < 0.05$ (two-tailed Student's *t*-test).

Statistical Analysis

Data were analyzed for statistical significance by using the Student's *t*-test. *P*-values lower than 0.05 were considered statistically significant.

RESULTS

Identification of the p70 Molecule and Induction by HCV

mAbs against RzM6-LC cells were screened, and the clone 2-243a, which recognizes p70, was obtained

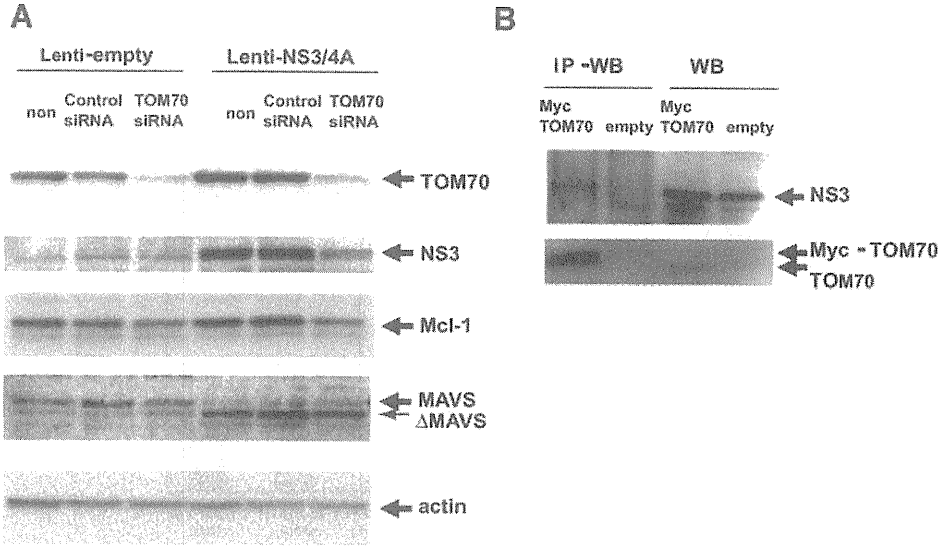

Fig. 3. Interaction between TOM70 and NS3 protein. A: The effect of TOM70 siRNA in cells transfected with empty or NS3/4A-containing lentivirus vectors was examined by WB with mAb 2-243a for TOM70; anti-NS3 rabbit polyclonal antibody; anti-Mcl-1 rabbit polyclonal antibody; anti-MAVS rabbit polyclonal antibody; and anti-actin antibody. B: The interaction between TOM70 and NS3 was assessed using IP-WB. NS3-expressing HepG2 cells were transfected with pcDNA6-TOM70 (mycTOM70) or pcDNA6 alone (empty) and immunoprecipitated with the anti-myc antibody (9E10). NS3 was detected using polyclonal rabbit anti-NS3 antibody (upper image), and TOM70 was detected using mAb 2-243a (lower image).

(Fig. 1A). p70 was induced to a greater extent by HCV expression after 8 days (RzM6-8d) or more than 44 days (RzM6-LC) than before HCV expression (RzM6-0d). The p70 expression level did not differ among the human hepatic cell lines (WRL68, HepG2, and HuH-7) (Fig. 1A, right panel). p70 was characterized (Fig. 1B–E): The sequence of peptides determined using MALDI-TOF-MS (Fig. 1B) and the MS/MS spectra of the p70 peptide sequence NVDLSTFYQNR (Fig. 1C) are provided. TOM70-pcDNA6 expression in HuH-7 cells was detected by WB with mAb 2-243a (Fig. 1D). Cell lysates were immunoprecipitated with anti-rat TOM70 antibody and detected by WB using mAb 2-243a (Fig. 1E). These results indicate that mAb 2-243a recognizes TOM70. Next, the effect of HCV infection on TOM70 expression was examined (Fig. 1F), and infection with the HCV JFH-1 strain [Wakita et al., 2005] induced TOM70 expression in HuH-7 cells (Fig. 1F). TOM70 localization was characterized using an indirect fluorescence assay (IFA) with 2-243a; anti-PDI, an ER marker; or MitoRed, which is a selective mitochondrial marker (Fig. 1G). TOM70 was associated with the mitochondria in all cells and was a part (~40%) of the ER, indicating that the TOM70 expressions in the mitochondria were higher than those in the ER.

TOM70 Inhibits TNF-α-Mediated Apoptotic Cell Death

The results of previous studies indicate the significant role of mitochondria in the apoptotic response [Hatano, 2007]. TOM70 interacts with Mcl-1 and facilitates mitochondrial targeting by the latter [Chou et al., 2006]. Mcl-1 silencing enhances TNF-related apoptosis-inducing ligand (TRAIL)-mediated cell death [Wirth et al., 2005; Han et al., 2006]. Therefore, the role of TOM70 in the apoptotic response was examined in this study. HepG2 cells were transfected with TOM70-pcDNA6 (Fig. 1D) or empty pcDNA6 (control), and their sensitivity to anti-Fas antibody (Fig. 2A) and TNF-α-mediated apoptotic cell death (Fig. 2B) was examined. When treated with 8 ng/ml of TNF-α, the TOM70-pcDNA6-transfected cells were significantly more viable than those transfected with empty pcDNA6 (Fig. 2B). In contrast, no significant differences were found between the viability of TOM70-pcDNA6 transfected cells and control cells treated with anti-Fas antibody (Fig. 2A). Thus, TNF-α-induced apoptosis was inhibited by TOM70 overexpression.

Interaction of TOM70 With HCV-NS3 and Other Host Factors

To determine the mechanism by which HCV induces TOM70, the TOM70 level in HCV NS3/4A-expressing HepG2 cells was determined (Fig. 3A). The TOM70 level was higher in the NS3/4A-expressing cells than in the control cells. Interestingly, the level of NS3/4A protein as well as Mcl-1 was reduced when TOM70 was silenced. The MAVS protein is cleaved by NS3/4A, as reported previously [Li et al., 2005], and the level of this protein was not influenced by the silencing of TOM70. IP-WB was performed to examine the possible interaction between TOM70 and NS3/4A (Fig. 3B). The pcDNA6-TOM70-myc plasmid was transfected into lenti-NS3/4A vector-transduced HepG2 cells; IP was performed using the anti-myc antibody, and the reaction was detected using the anti-NS3 antibody. The NS3 protein was

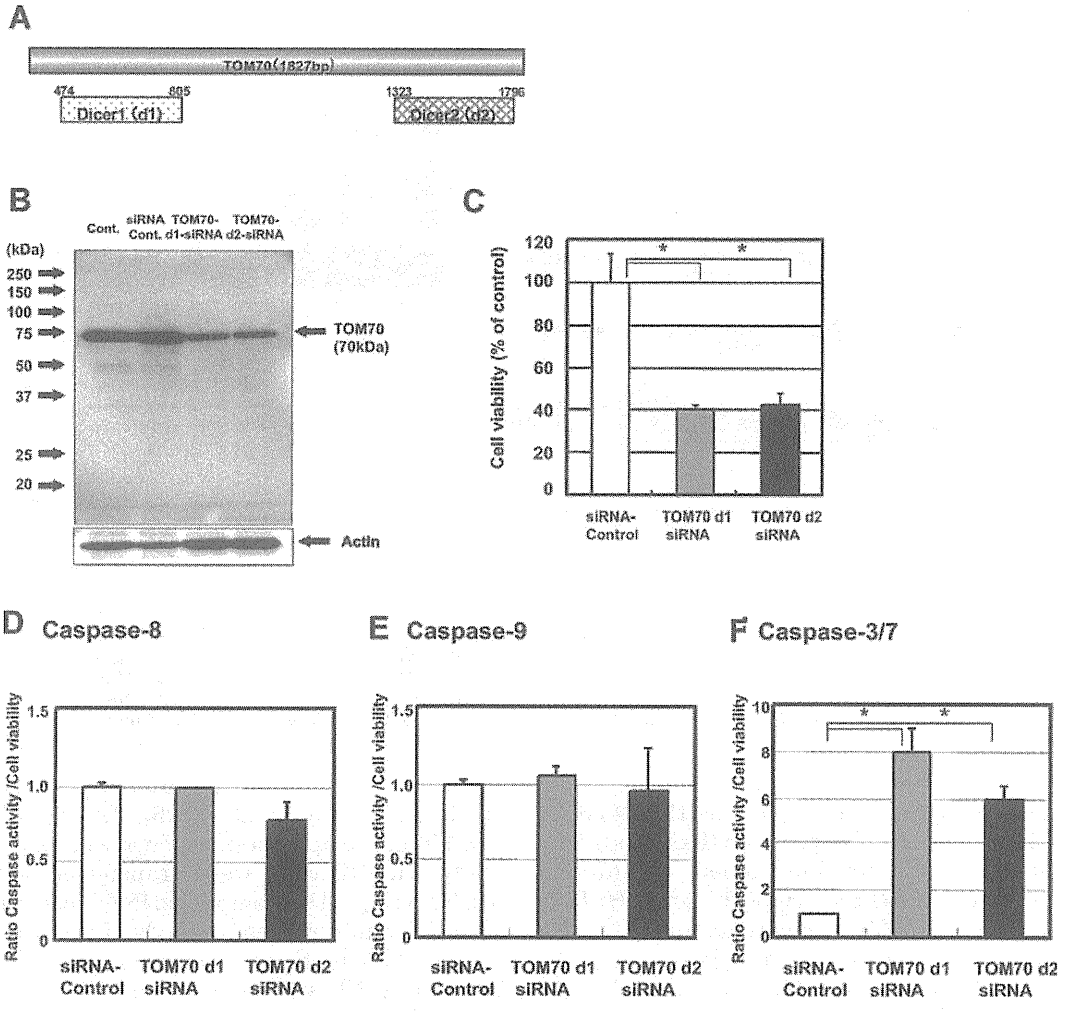

Fig. 4. Silencing of TOM70 induced apoptotic cell death and caspase-3/7 activity. A: The positions of TOM70-d1-siRNA and TOM70-d2-siRNA are indicated in the figure. B: siRNA-mediated silencing of TOM70 was detected by WB (Cont: no siRNA, siRNA Cont: siRNA control (Luci2-siRNA), TOM70-d1-siRNA, TOM70-d2-siRNA). C: TOM70 knockdown-induced cell death was calculated by measuring viability (%) with the WST-8 cell counting kit. The cell viability after 48 hr was scored in HepG2 cells transfected with the siRNA control Luci2-siRNA (□), TOM70-d1-siRNA (■), and TOM70-d2-siRNA (■). The activities of caspase-8 (**D**), caspase-9 (**E**), and caspase-3/7 (**F**) were measured using commercially available assays and a luminometer. The caspase activity was scored after 48 hr in TOM70-knockdown HepG2 cells transfected with control siRNA (□), TOM70-d1-siRNA (■), and TOM70-d2-siRNA (■). C–F: The data represent the average of the values obtained from triplicate experiments, and the vertical bars indicate the SD. $^{*}P < 0.05$ (two-tailed Student's *t*-test).

specifically precipitated by myc-tagged TOM70. The NS4A protein was not detected in this assay (data not shown). Therefore, the NS3 protein directly interacts with TOM70.

TOM70 Knockdown by RNAi Induces Apoptosis

The effect of TOM70 on the apoptotic response was examined because TOM70 silencing decreased the level of Mcl-1. First, two siRNAs for TOM70 (TOM70-d1-siRNA and TOM70-d2-siRNA) were designed in order to prevent the off-target effect (Fig. 4A). siRNA for luciferase (Luci-d2-siRNA) was used as a control (Fig. 4B). HepG2 cells were transfected with TOM70-d1-siRNA or TOM70-d2-siRNA, and the downregulation of TOM70 expression was confirmed by WB (Fig. 4B). Furthermore, decreased cell viability was observed (Fig. 4C) after 48 hr. Treatment with TOM70-d1-siRNA or TOM70-d2-siRNA significantly decreased the cell viability of HuH-7 cells too (data not shown). These results indicate that TOM70 silencing with siRNA may induce apoptosis.

The activities of caspase-3/7, caspase-8, and caspase-9 in HepG2 cells were examined after TOM70 silencing (Fig. 4D–F). The activities of caspase-8 and caspase-9 in cells transfected with TOM70 siRNA were not significantly different from those in the cells treated with control siRNA (Fig. 4D,E). In contrast, the caspase-3/7 activity in the TOM70-siRNA transfected cells was significantly greater than that in the cells treated with

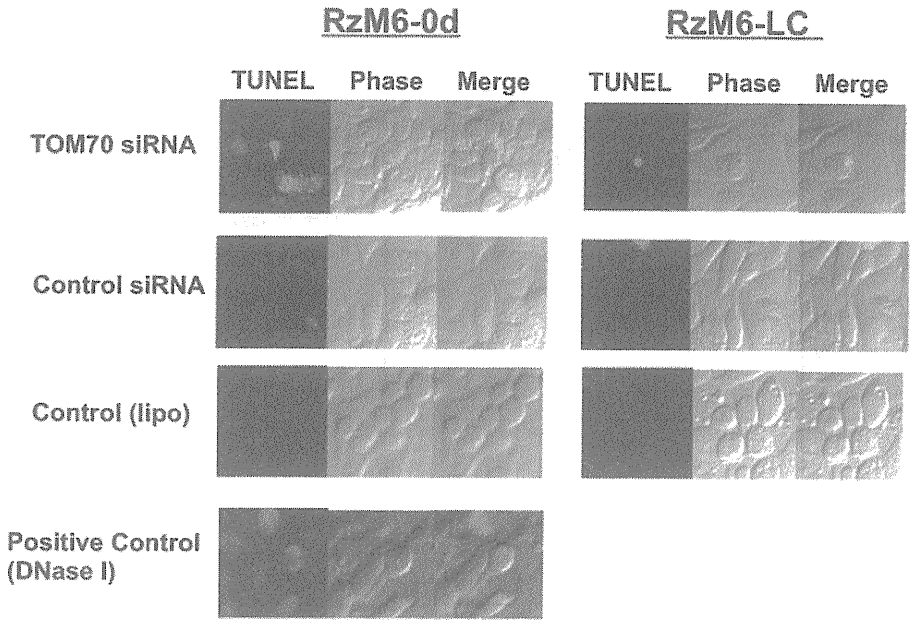

Fig. 5. TUNEL assay in RzM6-0d and RzM6-LC cells transfected with TOM70 siRNA, control siRNA, and control (Lipofectamine). The positive control is RzM6-0d cells treated with DNase I. The magnification is 400×.

control siRNA (Fig. 4F). These results indicate that the siRNA-mediated silencing of TOM70 expression induces apoptosis through caspase-3/7.

TOM70 Silencing-Induced Apoptosis Is Impaired by HCV

Next, the effect of TOM70 silencing-induced apoptosis was examined in RzM6-0d and RzM6-LC cells in order to determine the effect of HCV expression (Fig. 5). The apoptotic response was examined using the TUNEL assay wherein DNA strand breaks are detected and the apoptotic response is thereby detected [Gavrieli et al., 1992]. The DNA strand breaks, which were stained red, were observed using confocal microscopy. Treatment with TOM70 siRNA produced significant DNA strand breaks in the RzM6-0d cells. However, the apoptotic signal was suppressed in the RzM6-LC cells. This indicates the possibility that HCV can impair the apoptotic response induced by TOM70 siRNA.

Silencing of TOM70 Decreases Cell Viability, Whereas HCV-NS3 Restores Cell Viability

The RzM6-0d and RzM6-LC cells were treated with TOM70 siRNA and control siRNA, and the cell viability was measured using the WST-8 assay [Isobe et al., 1999] (Fig. 6A). The viability of the RzM6-LC cells was significantly higher than that of the RzM6-0d cells after treatment with TOM70 siRNA, and this difference increased in a dose-dependent manner. This indicates that the expression of HCV genes may impair the TOM70 siRNA-induced apoptotic response. The responsible HCV protein was identified using the lentivirus vector (Fig. 6B), and TOM70 siRNA-induced cell death was found to be impaired in HCV-NS3/4A-expressing cells.

DISCUSSION

The results of the present study suggest that HCV interacts with TOM70 through the NS3 protein, which indicates the possibility that TOM70 regulates the intracellular localization of HCV NS3; a previous study has reported the mitochondrion to be one of the regions where HCV NS3 is located [Sillanpaa et al., 2008]. The results of a previous study indicate that TOM70 also interacts with the Mcl-1 protein [Chou et al., 2006]. TOM70 silencing decreased the levels of the NS3 and Mcl-1 proteins; therefore, interaction with TOM70 may increase the stability of NS3 and Mcl-1. Recently, it was reported that Mcl-1 is stabilized by the deubiquitinase USP9X and that it can promote tumor cell survival [Schwickart et al., 2010]. Furthermore, Mcl-1 interacts with the HCV core protein through Bcl-2 homology domain 3 (BH3) [Mohd-Ismail et al., 2009], and Mcl-1 overexpression suppresses core-induced apoptosis. Therefore, further studies are required to clarify the relationship between TOM70, Mcl-1, and other host factors in HCV infection. This information may provide novel insights into the mechanism underlying the induction of apoptotic resistance and tumorigenicity in hepatocytes during chronic HCV infection.

The results of this study indicate the regulatory role of TOM70 in apoptosis. TOM70 overexpression was found to suppress the TNF-α-mediated but not the Fas-mediated apoptotic response. TOM70 knockdown

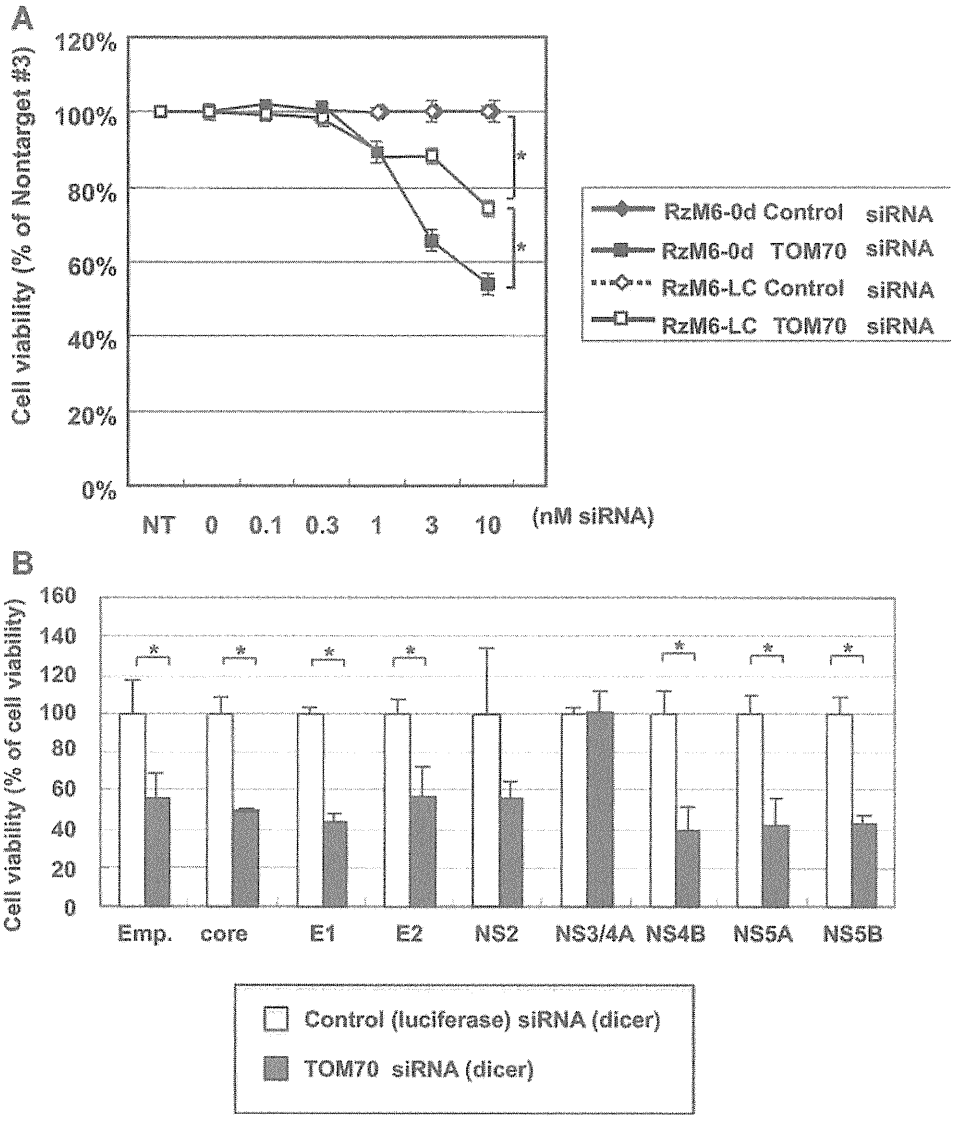

Fig. 6. A: Cell viability of RzM6-0d or RzM6-LC cells after treatment with TOM70 siRNA. The viability is given as the ratio (%) of test to control siRNA treatment. **B**: The viability of HepG2 cells transduced with lentivirus vectors expressing the HCV core, E1, E2, NS2, NS3/4A, NS4B, NS5A, and NS5B proteins after treatment with TOM70 siRNA was measured by the WST assay, and the viability is given as the ratio (%) of the test to the control siRNA treatment. The data represents the average of the values obtained from triplicate experiments, and the vertical bars indicate SD. $^{*}P < 0.05$ (two-tailed Student's *t*-test).

increased caspase-3/7 activity, but the activities of caspase-8 and caspase-9 were not significantly affected. This indicates the possibility that TOM70 regulates the TNF receptor-mediated apoptotic pathway. Several reports have indicated that TNF-α-mediated apoptosis is inhibited by HCV proteins. Saito et al. [2006] reported that the HCV core protein inhibited the TNF-α-mediated signaling pathway through the sustained expression of a cellular- FADD-like interleukin-1β-converting enzyme (FLICE) like inhibitory protein (c-FLIP; caspase-8 inhibitor). Majumder et al. [2002] reported that TNF-α-mediated hepatic apoptosis was impaired by the HCV-NS5A protein. The results of the present study revealed an alternative pathway by which HCV can acquire TNF-α-induced apoptotic resistance through TOM70 augmentation. Recently, it has been reported that TOM70 interacts with MAVS, TNFRSF1A-associated via death domain (TRADD), TNF receptor-associated factor 6 (TRAF6), stimulator of interferon genes (STING), and interferon regulatory factor (IRF)-3, and that augmentation of TOM70 activates retinoic acid-inducible gene (RIG)-I signaling [Liu et al., 2010]. The results of recent studies indicate that IRF-3 can activate Bax expression and apoptosis [Chattopadhyay et al., 2004]. Future studies on the modification of the regulatory pathway of TOM70 by HCV may provide further insights on the mechanism underlying persistent HCV infection.

ACKNOWLEDGMENTS

The authors thank Dr. H. Fukuda and Dr. S. Ohmi for their technical support with regard to MALDI-TOF-MS analysis, Dr. F. Yasui and Dr. T. Munakata for their critical comments, Dr. Satoh for his technical support, and Prof. S. Harada for his support.

REFERENCES

Chattopadhyay S, Marques JT, Yamashita M, Peters KL, Smith K, Desai A, Williams BR, Sen GC. 2004. Viral apoptosis is induced by IRF-3-mediated activation of Bax. EMBO J 29:1762–1773.

Chou CH, Lee RS, Yang-Yen HF. 2006. An internal EELD domain facilitates mitochondrial targeting of Mcl-1 via a Tom70-dependent pathway. Mol Biol Cell 17:3952–3963.

Deng L, Adachi T, Kitayama K, Bungyoku Y, Kitazawa S, Ishido S, Shoji I, Hotta H. 2008. Hepatitis C virus infection induces apoptosis through a Bax-triggered, mitochondrion-mediated, caspase 3-dependent pathway. J Virol 82:10375–10385.

Gavrieli Y, Sherman Y, Ben-Sasson SA. 1992. Identification of programmed cell death in situ via specific labeling of nuclear DNA fragmentation. J Cell Biol 119:493–501.

Han J, Goldstein LA, Gastman BR, Rabinowich H. 2006. Interrelated roles for Mcl-1 and BIM in regulation of TRAIL-mediated mitochondrial apoptosis. J Biol Chem 281:10153–10163.

Hatano E. 2007. Tumor necrosis factor signaling in hepatocyte apoptosis. J Gastroenterol Hepatol 22:S43–S44.

Hoogenraad NJ, Ward LA, Ryan MT. 2002. Import and assembly of proteins into mitochondria of mammalian cells. Biochim Biophys Acta 1592:97–105.

Isobe I, Michikawa M, Yanagisawa K. 1999. Enhancement of MTT, a tetrazolium salt, exocytosis by amyloid beta-protein and chloroquine in cultured rat astrocytes. Neurosci Lett 266:129–132.

Jensen ON, Wilm M, Shevchenko A, Mann M. 1999. Sample preparation methods for mass spectrometric peptide mapping directly from 2-DE gels. Methods Mol Biol 112:513–530.

Lei Y, Moore CB, Liesman RM, O'Connor BP, Bergstralh DT, Chen ZJ, Pickles RJ, Ting JP. 2009. MAVS-mediated apoptosis and its inhibition by viral proteins. PLoS One 4:e5466.

Li XD, Sun L, Seth RB, Pineda G, Chen ZJ. 2005. Hepatitis C virus protease NS3/4A cleaves mitochondrial antiviral signaling protein off the mitochondria to evade innate immunity. Proc Natl Acad Sci USA 102:17717–17722.

Liu XY, Wei B, Shi HX, Shan YF, Wang C. 2010. Tom70 mediates activation of interferon regulatory factor 3 on mitochondria. Cell Res 20:994–1011.

Majumder M, Ghosh AK, Steele R, Zhou XY, Phillips NJ, Ray R, Ray RB. 2002. Hepatitis C virus NS5A protein impairs TNF-mediated hepatic apoptosis, but not by an anti-FAS antibody, in transgenic mice. Virology 294:94–105.

Mihara K, Omura T. 1996. Cytoplasmic chaperones in precursor targeting to mitochondria: The role of MSF and hsp 70. Trends Cell Biol 6:104–108.

Mohd-Ismail NK, Deng L, Sukumaran SK, Yu VC, Hotta H, Tan YJ. 2009. The hepatitis C virus core protein contains a BH3 domain that regulates apoptosis through specific interaction with human Mcl-1. J Virol 83:9993–10006.

Neupert W. 1997. Protein import into mitochondria. Annu Rev Biochem 66:863–917.

Nishimura T, Kohara M, Izumi K, Kasama Y, Hirata Y, Huang Y, Shuda M, Mukaidani C, Takano T, Tokunaga Y, Nuriya H, Satoh M, Saito M, Kai C, Tsukiyama-Kohara K. 2009. Hepatitis C virus impairs p53 via persistent overexpression of 3beta-hydroxysterol Delta24-reductase. J Biol Chem 284:36442–36452.

Nomura-Takigawa Y, Nagano-Fujii M, Deng L, Kitazawa S, Ishido S, Sada K, Hotta H. 2006. Non-structural protein 4A of Hepatitis C virus accumulates on mitochondria and renders the cells prone to undergoing mitochondria-mediated apoptosis. J Gen Virol 87:1935–1945.

Pfanner N, Geissler A. 2001. Versatility of the mitochondrial protein import machinery. Nat Rev Mol Cell Biol 2:339–349.

Pfanner N, Meijer M. 1997. The Tom and Tim machine. Curr Biol 7:R100–R103.

Saito K, Meyer K, Warner R, Basu A, Ray RB, Ray R. 2006. Hepatitis C virus core protein inhibits tumor necrosis factor alpha-mediated apoptosis by a protective effect involving cellular FLICE inhibitory protein. J Virol 80:4372–4379.

Saitou K, Mizumoto K, Nishimura T, Kai C, Tsukiyama-Kohara K. 2009. Hepatitis C virus-core protein facilitates the degradation of Ku70 and reduces DNA-PK activity in hepatocytes. Virus Res 144:266–271.

Schatz G. 1996. The protein import system of mitochondria. J Biol Chem 271:31763–31766.

Schwickart M, Huang X, Lill JR, Liu J, Ferrando R, French DM, Maecker H, O'Rourke K, Bazan F, Eastham-Anderson J, Yue P, Dornan D, Huang DC, Dixit VM. 2010. Deubiquitinase USP9X stabilizes MCL1 and promotes tumour cell survival. Nature 463:103–107.

Seeff LB. 2002. Natural history of chronic hepatitis C. Hepatology 36:S35–S46.

Sillanpaa M, Kaukinen P, Melen K, Julkunen I. 2008. Hepatitis C virus proteins interfere with the activation of chemokine gene promoters and downregulate chemokine gene expression. J Gen Virol 89:432–443.

Stojanovski D, Johnston AJ, Streimann I, Hoogenraad NJ, Ryan MT. 2003. Import of nuclear-encoded proteins into mitochondria. Exp Physiol 88:57–64.

Truscott KN, Pfanner N, Voos W. 2001. Transport of proteins into mitochondria. Rev Physiol Biochem Pharmacol 143:81–136.

Tsukiyama-Kohara K, Tone S, Maruyama I, Inoue K, Katsume A, Nuriya H, Ohmori H, Ohkawa J, Taira K, Hoshikawa Y, Shibasaki F, Reth M, Minatogawa Y, Kohara M. 2004. Activation of the CKI-CDK-Rb-E2F pathway in full genome hepatitis C virus-expressing cells. J Biol Chem 279:14531–14541.

Wakita T, Pietschmann T, Kato T, Date T, Miyamoto M, Zhao Z, Murthy K, Habermann A, Krausslich HG, Mizokami M, Bartenschlager R, Liang TJ. 2005. Production of infectious hepatitis C virus in tissue culture from a cloned viral genome. Nat Med 11:791–796.

Wirth T, Kuhnel F, Fleischmann-Mundt B, Woller N, Djojosubroto M, Rudolph KL, Manns M, Zender L, Kubicka S. 2005. Telomerase-dependent virotherapy overcomes resistance of hepatocellular carcinomas against chemotherapy and tumor necrosis factor-related apoptosis-inducing ligand by elimination of Mcl-1. Cancer Res 65:7393–7402.

International Scholarly Research Network
ISRN Hematology
Volume 2011, Article ID 167501, 8 pages
doi:10.5402/2011/167501

Review Article

Hepatitis C Virus-Related Lymphomagenesis in a Mouse Model

Kyoko Tsukiyama-Kohara,[1] Satoshi Sekiguchi,[2] Yuri Kasama,[1] Nagla Elwy Salem,[1,3,4] Keigo Machida,[5] and Michinori Kohara[2]

[1] *Department of Experimental Phylaxiology, Faculty of Life Sciences, Kumamoto University, 1-1-1 Honjo, Kumamoto-shi, Kumamoto 860-8556, Japan*
[2] *Department of Microbiology and Cell Biology, The Tokyo Metropolitan Institute of Medical Science, 2-1-6 Kamikitazawa, Setagaya-ku, Tokyo 156-8506, Japan*
[3] *Department of Medical Virology, Faculty of Life Sciences, Kumamoto University, 1-1-1 Honjo, Kumamoto-shi, Kumamoto 860-8556, Japan*
[4] *Clinical Pathology Department, Faculty of Medicine, Suez Canal University, Round Road Kilo 4.5, Ismailia, Egypt*
[5] *Department of Molecular Microbiology and Immunology, University of Southern California, Keck School of Medicine, Los Angeles, CA 90033, USA*

Correspondence should be addressed to Kyoko Tsukiyama-Kohara, kkohara@kumamoto-u.ac.jp

Received 5 May 2011; Accepted 2 June 2011

Academic Editors: D. Efremov and L. Visser

Copyright © 2011 Kyoko Tsukiyama-Kohara et al. This is an open access article distributed under the Creative Commons Attribution License, which permits unrestricted use, distribution, and reproduction in any medium, provided the original work is properly cited.

B cell non-Hodgkin lymphoma is a typical extrahepatic manifestation frequently associated with hepatitis C virus (HCV) infection. The mechanism by which HCV infection leads to lymphoproliferative disorder remains unclear. Our group established HCV transgenic mice that expressed the full HCV genome in B cells (RzCD19Cre mice). We observed a 25.0% incidence of diffuse large B cell non-Hodgkin lymphomas (22.2% in male and 29.6% in female mice) within 600 days of birth. Interestingly, RzCD19Cre mice with substantially elevated serum-soluble interleukin-2 receptor α-subunit (sIL-2Rα) levels (>1000 pg/mL) developed B cell lymphomas. Another mouse model of lymphoproliferative disorder was established by persistent expression of HCV structural proteins through disruption of interferon regulatory factor-1 (*irf-1*$^{-/-}$/CN2 mice). *Irf-1*$^{-/-}$/CN2 mice showed extremely high incidences of lymphomas and lymphoproliferative disorders. Moreover, these mice showed increased levels of interleukin (IL)-2, IL-10, and Bcl-2 as well as increased Bcl-2 expression, which promoted oncogenic transformation of lymphocytes.

1. Introduction

The incidence of non-Hodgkin lymphoma (NHL) is rising worldwide and is higher in developed countries than in Africa and Asia [1]. B cell non-Hodgkin lymphoma is a typical extrahepatic manifestation frequently associated with hepatitis C virus (HCV) infection [2]. The prevalence of HCV infection in patients with B cell non-Hodgkin lymphoma is approximately 15% [3]. The HCV envelope protein E2 binds human CD81 [4], a tetraspanin expressed on various types of cells, including lymphocytes, and activates B cell proliferation [5]. Infection and replication of HCV were observed in B cells [6, 7] although the direct effects, particularly *in vivo*, have not been clarified. To determine the direct effect of HCV infection on B cells *in vivo*, we crossed transgenic mice with an integrated full-length HCV genome (Rz) under the conditional Cre/*lox*P expression system, with mice expressing the Cre enzyme [8] under transcriptional control of the B lineage-restricted gene *CD19* [9].

To investigate the mechanism of development of lymphoproliferation or B cell non-Hodgkin lymphoma in HCV patients, we also developed a transgenic mouse model that conditionally expressed HCV cDNA (nucleotides 294–3435), including the viral genes that encode the core, E1, E2, and NS2 proteins, by using the Cre/*lox*P system (in core-NS2 [CN2] mice) [10, 11]. Conditional transgene activation of the HCV cDNA (core, E1, E2, and NS2) protects mice from Fas-mediated lethal acute liver failure, by inhibiting cytochrome *c* release from mitochondria [11]. Persistent HCV protein expression is established by targeted disruption

of interferon regulatory factor-1 (*irf-1*), and high incidences of lymphoproliferative disorders are noted in *irf-1*$^{-/-}$ CN2 mice [12].

Previously, transgenic mice that expressed the HCV core protein were established using a promoter derived from hepatitis B virus [13], whereas mice that expressed structural or complete viral proteins were established using promoters derived from the albumin gene [14]. These mice were immunotolerant to the transgene and did not develop hepatic inflammation. However, they developed age-related hepatic steatosis and hepatocellular carcinomas. In contrast, the CN2 mice used in the present study were not immunotolerant to the *HCV* gene and developed hepatitis after the onset of HCV gene expression. However, the expression of *HCV* in these mice was usually lost after 21 days. Therefore, an animal model of persistent HCV protein expression is required for examining the effects of chronic HCV infection *in vivo*.

IFN signaling mediates tumor-suppressor effects and antiviral responses and is regulated by key transcription factors of the interferon-regulatory factor (IRF) protein family, including IRF1, IRF2, IRF3, IRF7, and IRF9. Targeted disruption of *irf-1* results in aberrant lymphocyte development and a marked reduction in the number of CD8$^+$ T cells in the peripheral blood, spleen, and lymph nodes [15]. In addition, natural killer cell development is impaired in *irf-1*$^{-/-}$ mice [16]. The mechanisms by which HCV infection induces IFN resistance and influences the development of lymphomas are poorly understood. Therefore, we established an *irf-1*$^{-/-}$ CN2 mouse model of persistent HCV expression, which allowed us to investigate the effects of HCV on lymphatic tissue tumor development.

2. Spontaneous Development of B Cell Lymphomas in the RzCD19Cre Mouse

The full-genome HCV expression was induced by the Cre/*lox*P system with CD19Cre (Figure 1(A)). Expression of HCV was mainly induced in B cells (Figure 1(B)). The incidence of B cell lymphomas in RzCD19Cre mice was 25.0% (22.2% in male and 29.6% in female mice) and was significantly higher than the incidence in the HCV-negative groups. Lymphomas were diagnosed as typical diffuse B cell non-Hodgkin lymphomas. Most were CD45R positive and located in the mesenteric lymph nodes (Figure 1(C)). Some were identified as intrahepatic lymphomas (incidence, 4.2%). *HCV* expression was detected in all B cell lymphomas of RzCD19Cre mice. Indeed, the expression of the *HCV* or HCV proteins induces the spontaneous development of B cell lymphomas, irrespective of the integrated site in the mouse genome.

Serum concentrations of IL-1α, IL-1β, IL-2, IL-3, IL-4, IL-5, IL-6, IL-9, IL-10, IL-12(p40), IL-12(p70), IL-13, IL-17, eotaxin, G-CSF, GM-CSF, IFN-γ, KC, MCP-1, MIP-1α, MIP-1β, RANTES, TNF-α, IL-15, FGF-basic, LIF, M-CSF, MIG, MIP-2, PDGFβ, VEGF, alanine aminotransferase (ALT), and aspartate aminotransferase (AST) were not significantly different in the presence or absence of B cell lymphomas. Interestingly, the average sIL-2Rα level was significantly higher in the sera from RzCD19Cre mice with B cell lymphomas (830.3 $\pm$ 533.0 pg/mL) than in that from tumor-free control groups, including the RzCD19Cre, Rz, CD19Cre, and wild-type (WT) mice (499.9 $\pm$ 110.2 pg/mL; $P < 0.0057$) (Figure 1(D)). The difference in the average sIL-2Rα levels between the sera from groups with tumors other than B cell lymphomas (430.46 $\pm$ 141.15 pg/mL) and that from tumor-free control groups was insignificant ($P > 0.05$). Moreover, all RzCD19Cre mice with a relatively high level of sIL-2Rα (>1000 pg/mL) presented with B cell lymphomas. A significant increase in sIL-2Rα was also observed in MxCre/CN2-29 mice that expressed the HCV CN2 gene [8] and had B cell lymphomas, compared with tumor-free control (CN2-29) mice.

To examine whether sIL-2Rα was derived from lymphoma tissues, we quantified IL-2Rα concentrations in splenocytes, peripheral blood lymphocytes (PBLs), and B cell lymphoma tissues. The concentration of IL-2Rα was significantly higher in splenocytes from RzCD19Cre mice than in splenocytes from CD19Cre mice. Moreover, the concentration of IL-2Rα in B cell lymphoma tissues from RzCD19Cre mice was higher than that in splenocytes [8]. These results strongly suggest that B cell lymphomas directly contribute to the elevated serum concentrations of sIL-2Rα in RzCD19Cre mice. They also strongly support the possibility that persistent expression of HCV could directly induce transformation of B cells.

3. Persistent HCV Expression and Lymphoproliferative Disorder

RzCD19Cre mice are immunotolerant to HCV, because *HCV* is expressed in B cells before birth. In contrast, CN2 mice express *HCV* after they are administered the recombinant adenovirus that expresses the Cre enzyme (Figures 2(a) and 2(b)). The expression of HCV in these mice is usually lost after 21 days (Figure 2(b)) through removal of HCV-expressing hepatocytes by the immune response. To establish persistent HCV expression, we disrupted *irf-1* by crossing of RzCD19Cre mice with *irf-1*$^{-/-}$ mice. IRF-1 plays a significant role in the Th1-type immune response and its absence is expected to decrease the elimination of HCV-expressing cells. As expected, HCV expression in *irf-1*$^{-/-}$ CN2 mice persisted for more than 500 days (Figure 2(c)).

A significant percentage of the mice that expressed the HCV core protein (*irf-1*$^{-/-}$ CN2 mice) showed polyclonal lymphoid growth disturbances, including splenomegaly, expanded lymph nodes, adenocarcinoma in the abdomen or leg, and lymphoma of the liver or Peyer's patches (Figures 2(d) and 2(e)). In contrast, hepatocytes with abundant expression of HCV proteins rarely developed into hepatocellular carcinomas. Hematoxylin and eosin (H&E) staining of splenomegalic tissue showed extensive hyperplasia of the white pulp zones, in which the cortical zones contained lymphoid follicles and scattered germinal centers although mitotic figures were rarely observed. These results indicate that persistent expression of HCV proteins frequently induces lymphoproliferative disorders in addition to liver

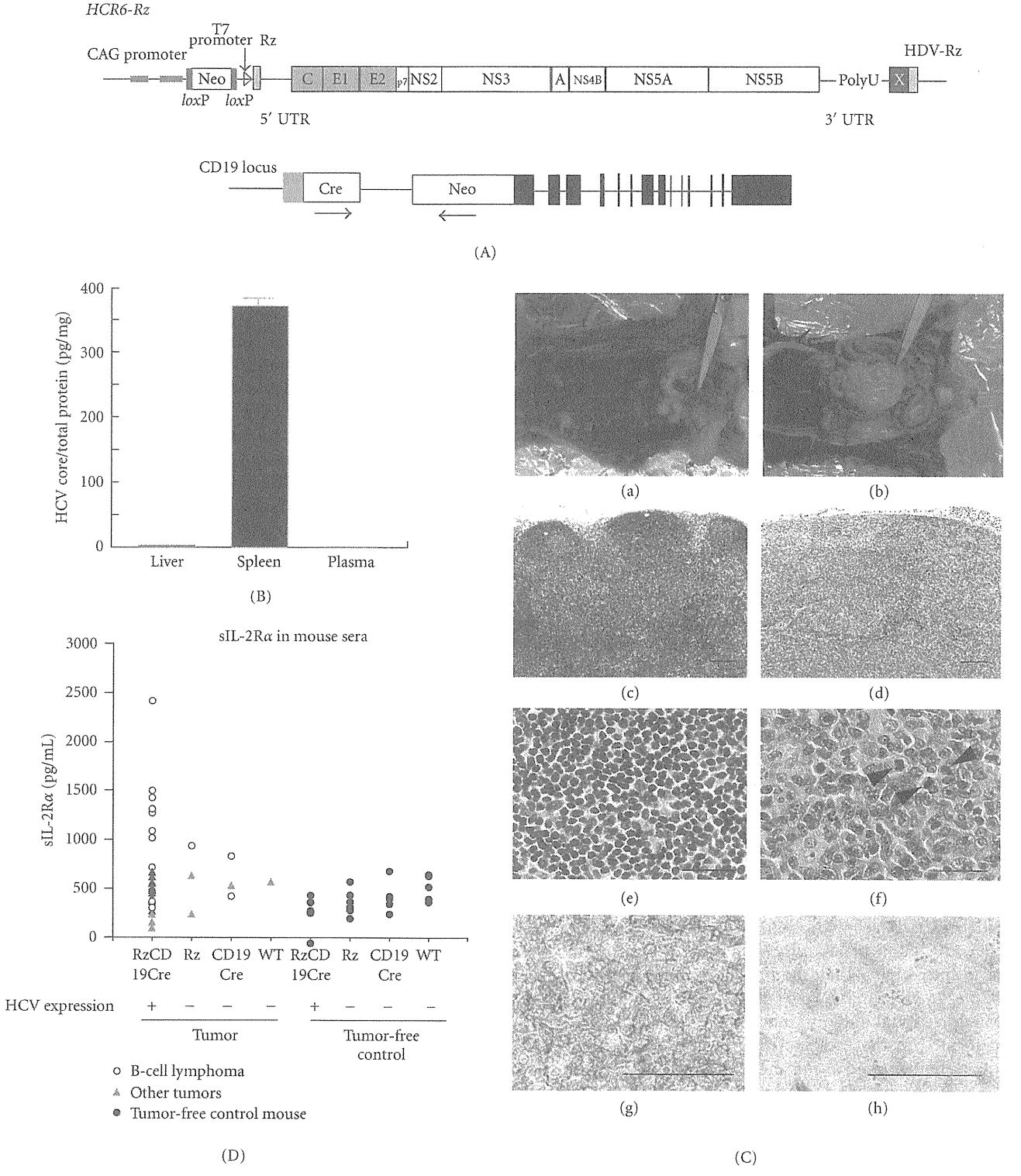

FIGURE 1: (A) The structure of the hepatitis C virus (HCV) transgene (HCR6-Rz); *HCV* gene expression was regulated by the Cre/*lox*P expression cassette (upper). The Cre transgene was located in the CD19 locus (bottom). (B) Expression of HCV core protein in the liver, spleen, and plasma of RzCD19Cre mice was quantified by core ELISA. Data represent the mean (SD) ($n = 3$). (C) Histological analysis of tissues from a normal mouse (a, c, e; lymph node from CD19Cre mouse; b, d, f) and B cell lymphoma (b, d, f; RzCD19Cre mouse). Paraformaldehyde-fixed and paraffin-embedded tumor tissues were stained with hematoxylin and eosin (H&E) (c–f); immunostaining of lymphoma with anti-CD45R (g) and anti-CD3 (h) is indicated. Scale bars, 100 μm (c, d) and 20 μm (g, h); arrow heads indicate mitotic cells. (D) Concentration of sIL-2Rα in serum samples from tumor-free control mice, and RzCD19Cre and wild-type (WT) mice with or without B-cell lymphomas or other tumors.

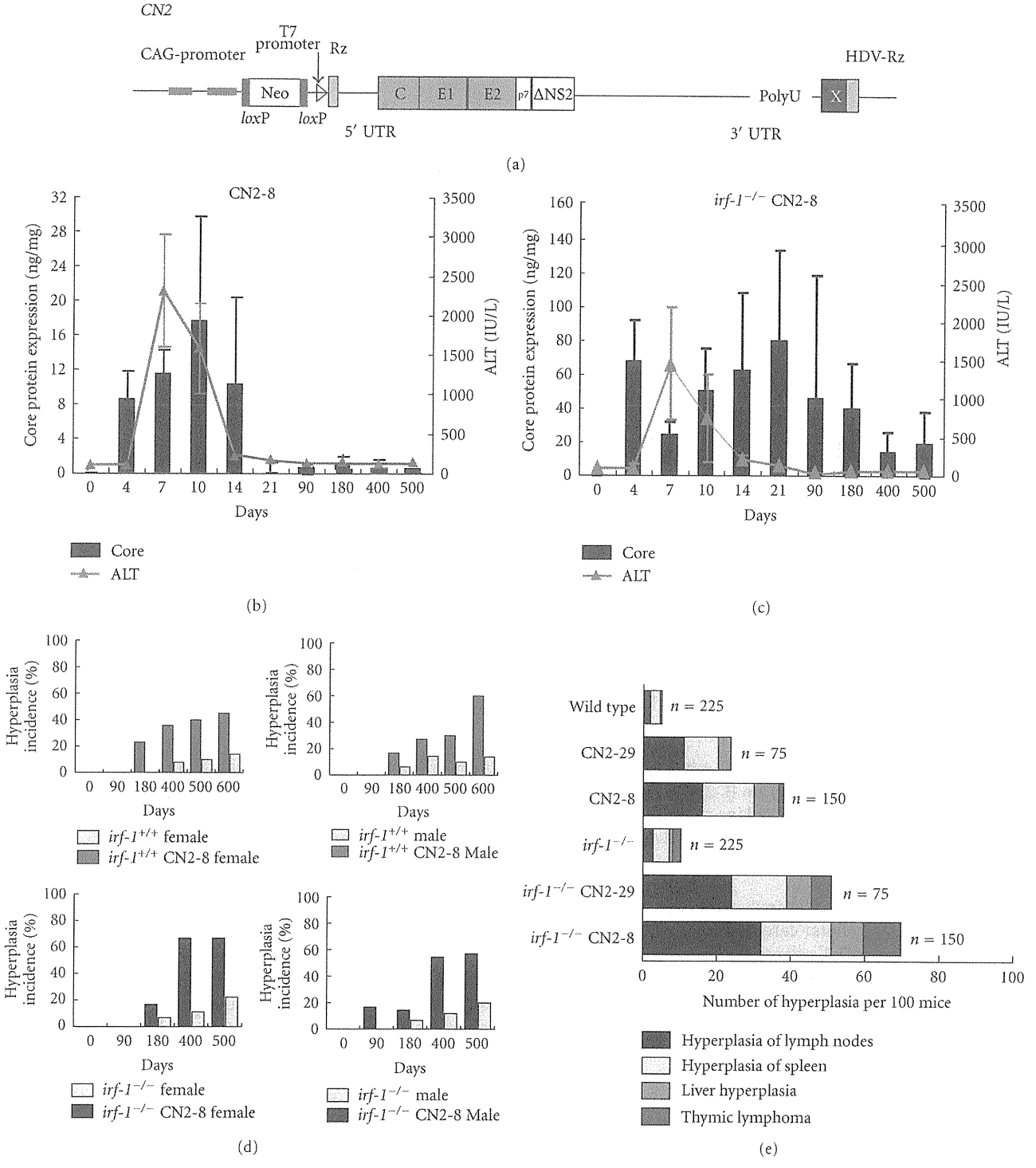

FIGURE 2: (a) The structure of the HCV transgene (core-NS2); gene expression was regulated by the Cre/*lox*P expression cassette. (b) and (c) Serum alanine aminotransferase (ALT) levels and core protein expression ELISA system in hepatocytes from CN2-8 (b) and *irf-1*$^{-/-}$ CN2-8 (c) mice after administration of AxCANCre (n = 225 for *irf-1*$^{-/-}$, n = 75 for *irf-1*$^{-/-}$ CN2-29, n = 150 for *irf-1*$^{-/-}$ CN2-8, n = 225 for wild type, n = 75 for CN2-29, and n = 150 for CN2-8; total n = 900). (d) HCV protein expression enhanced hyperplasia in male and female CN2 and *irf-1*$^{-/-}$ CN2 mice. The occurrence of hyperplasia was monitored every 7 days for 600 days after administration of AxCANCre. (e) Histological analysis of spontaneous proliferative disturbances in CN2 transgenic mice. Of the 900 mice injected with AxCANCre, 25 of 75 (33%) CN2-29, 47 of 150 (31%) CN2-8, 29 of 75 (39%) *irf-1*$^{-/-}$ CN2-29, and 62 of 150 (41%) *irf-1*$^{-/-}$ CN2-8 mice developed proliferative disturbances.

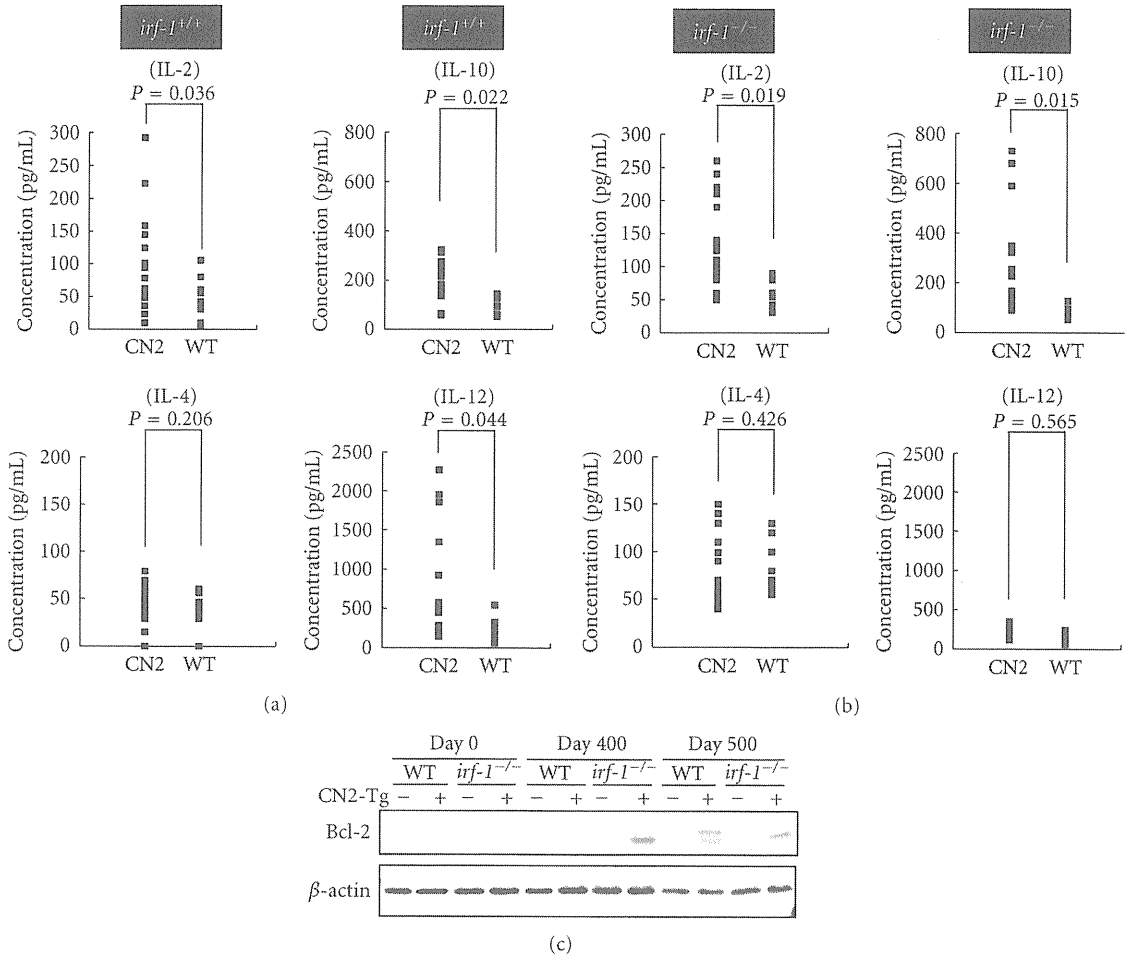

FIGURE 3: (a) Serum IL-2, IL-4, IL-10, and IL-12 levels in *irf-1*$^{+/+}$ CN2 (Tg+) and *irf-1*$^{+/+}$ WT mice measured by ELISA. P values <0.05 were considered significant. (b) Serum IL-2, IL-4, IL-10, and IL-12 levels in *irf-1*$^{-/-}$ CN2 (Tg+) and *irf-1*$^{-/-}$ WT mice measured by ELISA. P values are based on the mean cytokine concentrations. (c) Bcl-2 protein levels in the lymph nodes of *irf-1*$^{+/+}$ WT and *irf-1*$^{-/-}$ WT or transgenic (CN2-29) mice on day 0, day 400, and day 500 after administration of AxCANCre. Bcl-2 migrated at 26 kD.

hyperplasia, which is consistent with the phenotype of patients with hepatocellular carcinoma.

The average ratio of T cells to B cells in the lymph nodes and spleens of CN2 mice was significantly higher than that in WT mice. The majority of CD3$^+$ lymphocytes and a few CD8$^+$ lymphocytes expressed CD4 on their surfaces. The proliferating cells were mainly CD4$^+$ T cells although some were CD45R$^+$B cells. The *irf-1*$^{-/-}$ CN2 mice also developed B cell lymphomas (data not shown). These results confirm that HCV protein expression induces lymphoproliferative disorders that involve excessive expansion of both T cells and B cells. The cell population that showed negative results for T cell receptor (α, β, γ, and δ isoforms) staining was smaller in *irf-1*$^{-/-}$ CN2 mice than that in the other mice.

The disruption of *irf-1* inhibited Fas-induced apoptosis, presumably by decreasing the levels of caspase-6 and caspase-7 messenger RNA. These results suggest that the reduced expression of effector caspases delays Fas-mediated apoptosis in *irf-1*$^{-/-}$ mice and prevents the elimination of HCV-expressing cells *in vivo*.

The CN2 mice showed significantly increased levels of serum IL-2, IL-10, and IL-12 (Figure 3(a)). Notably, the CN2 mice with proliferative disturbances in the lymph nodes and spleen had dramatically elevated levels of these cytokines, suggesting that altered cytokine production is involved in aberrant lymphocyte proliferation or differentiation. In contrast, the *irf-1*$^{-/-}$ CN2 mice did not show elevated levels of serum IL-12, but had significantly higher levels of serum IL-2 and IL-10 than did *irf-1*$^{-/-}$ mice (Figure 3(b)). Thus, the disruption of *irf-1* negated the increase in the IL-12 level, but augmented the increases in the levels of IL-2 and IL-10 in CN2 mice. These results indicate that IL-2 and IL-10 play key roles in the induction of the lymphoproliferative phenotype in *irf-1*$^{-/-}$ CN2 mice. A significantly positive correlation was found between the cytokine levels and spleen weights of *CN2* gene-expressing mice with the *irf-1*$^{+/+}$ background (R = 0.43, P < 0.05, and R = 0.53, P < 0.05, resp.). These results indicate that IL-2 and IL-10 are involved in lymphoproliferation in viral protein-expressing mice.

Bcl-2 is an integral inner mitochondrial membrane protein, overexpression of which blocks the apoptotic death

Table 1: Synergistic effects of cytokines on Fas-induced apoptosis in *irf-1*$^{-/-}$ CN2 mice.

	None	IL-2 + IL-10	IL-2 + IL-12	IL-10 + IL-12
		WT mice		
Bcl-2 fold increase	−	−	−	−
Annexin V + percentage	****	****	****	****
Caspase-9	**	**	**	**
Caspase-3/7	***	***	***	***
		irf-1$^{-/-}$ mice		
Bcl-2 fold increase	−	−	−	−
Annexin V + percentage	***	***	***	***
Caspase-9	**	**	**	**
Caspase-3/7	**	**	**	**
		CN2-29 mice		
Bcl-2 fold increase	−	+	−	−
Annexin V + percentage	***	**	***	***
Caspase-9	**	*	*	**
Caspase-3/7	**	*	*	*
		irf-1$^{-/-}$ CN2-29 mice		
Bcl-2 fold increase	+	+++	++	++
Annexin V + percentage	**	−	*	*
Caspase-9	**	−	*	*
Caspase-3/7	*	−	*	*

Bcl-2: −, less than 2-fold increase; +, more than 2-fold increase; ++, more than 4-fold increase; +++, more than 6-fold increase (in comparison with mock treatment).
Annexin V: −, less than 20% decrease; *, up to 20% decrease; **, up to 40% decrease; ***, up to 60% decrease; ****, more than 60% decrease (in comparison with mock treatment).
Caspase-9: −, less than 10-fold decrease; *, up to 50-fold decrease; **, up to 200-fold decrease; ***, up to 400-fold decrease; ****, more than 400-fold decrease (in comparison with mock treatment).
Caspase-3/7: −, less than 200-fold decrease; ∗, up to 500-fold decrease; **, up to 1000-fold decrease; ***, more than 1000-fold decrease (in comparison with mock treatment).

of pro-B-lymphocyte death [17]. *Bcl-2* transgene expression increases the oncogenic potential [18] and is linked with B cell neoplasm and t(14;18) translocation [19]. We therefore examined the level of Bcl-2 protein and found that it was upregulated in the lymph nodes of *irf-1*$^{-/-}$ CN2 mice after 400 days (Figure 3(c)).

IL-10 treatment in the presence of IL-2 greatly inhibited Fas-induced apoptosis in *irf-1*$^{-/-}$ CN2 mice compared with other groups (Table 1). Furthermore, *irf-1* disruption accelerated the resistance of splenocytes to Fas-induced apoptosis in the presence of IL-2, IL-10, and/or IL-12. In particular, IL-2 plus IL-10 treatment produced the strongest upregulation of the Bcl-2 mRNA levels in splenocytes of *irf-1*$^{-/-}$ CN2 mice. This indicates that IL-2, IL-10, and/or IL-12 contribute to upregulation of *bcl-2* expression, which subsequently inhibits Fas-induced apoptosis. Caspase-9 and caspase-3/7 activities were inversely correlated with the level of *bcl-2* expression. These results indicate that aberrant cytokine expression and disruption of IFN signaling affect *bcl-2* expression synergizing with HCV proteins, which is associated with the inhibition of caspase expression.

Table 2: Synergistic effects of cytokines on Bcl-2 expression in WT and *irf-1*$^{-/-}$ mice in the presence of HCV core protein.

	WT mice	*irf-1*$^{-/-}$ mice
Mock	−	−
IL-2 + IL-10	+	+++
IL-2 + IL-12	+	++
IL-10 + IL-12	+	++
IL-2	−	−
IL-10	+	++
IL-12	−	−
IL-2 + Il-10 + IL-12	−	+

Bcl-2: −, less than 2-fold increase; +, more than 2-fold increase; ++, more than 4-fold increase; +++, more than 5-fold increase (in comparison with mock treatment).

HCV core protein induced IL-2 and IL-10. Envelope protein E2 induced IL-12 expression. These results indicate that the HCV core and E2 proteins are responsible for IL-2, IL-10, and IL-12 expression. Core protein expression and IL-10 stimulation most strongly induced Bcl-2 expression

(Table 2). From these results, core protein contributes significantly to the induction of Bcl-2 in the presence of cytokines.

4. Conclusion

Our results show that the conditional expression of HCV proteins induces inflammation and lymphoproliferative disorders. Furthermore, established animal models will probably provide critical information for the elucidation of the molecular mechanism(s) underlying the spontaneous development of B cell non-Hodgkin lymphoma after HCV infection. The disruption of *irf-1* enhances lymphoproliferative disorders. Therefore, IRF-1-inducible genes probably play essential roles in suppressing HCV-induced lymphoma and in eliminating HCV protein-expressing cells. The overexpression of apoptosis-related proteins (including Bcl-2) and/or aberrant cytokine production are the primary events in HCV-induced lymphoproliferation.

The *HCV* gene has the potential to induce B cell lymphomas in RzCD19Cre mice, without inducing host immune responses against *HCV* gene product. This is in agreement with the results of a previous study, which indicate that viral elimination reduces the incidence of malignant lymphoma in patients infected with HCV [20]. The incidence of B cell lymphoma in the HCV transgenic mouse strain (MxCre/CN2-29) is high, and this strongly suggests that development of B cell lymphomas occurs via expression of the *HCV* transgene.

Recent findings indicate a link between sIL-2Rα levels and hepatocellular carcinoma in Egyptian patients [21]. The level of IL-2Rα was higher in splenocytes of RzCD19Cre mice than in those of CD19Cre mice; however, the differences in the serum concentrations of sIL-2Rα between RzCD19Cre mice without B cell lymphomas and other control groups (Rz, CD19Cre, and WT) were insignificant. These results indicate that HCV increases IL-2Rα expression in B cells; proteolytic cleavage of IL-2Rα increased after B cell lymphoma development in the RzCD19Cre mice. The detailed mechanism by which HCV expression induces IL-2Rα remains unclear, but HCV core protein induces IL-10 expression in mouse splenocytes [12]. IL-10 upregulates the expression of IL-2Rα (Tac/CD25) in normal and leukemic B lymphocytes [22]. Therefore, through IL-10, the HCV core protein might induce IL-2Rα in B cells of the RzCD19Cre mouse.

Disruption of *irf-1* enables the persistent expression of HCV protein. This leads to lymphoproliferative diseases resulting from reduced apoptosis (i.e., lower levels of caspase-1, caspase-6, and caspase-7 expression). HCV CN2 transgenic (Tg+) mice are resistant to Fas-induced apoptosis because of the inhibition of cytochrome *c* release from mitochondria [11]. Mice with disruption of *irf-1* have several defects in their innate and adaptive immunities, including lineage-specific defects in thymocyte development, and the development of immature T cells into mature $CD4^+$ cells but not $CD8^+$ T cells [16, 23]. IRF-1 controls the positive and negative selection of $CD8^+$ thymocytes [24] and is required for the development of the Th1-type immune response. The absence of IRF-1 induces Th2-type immune response [16, 25]. The number of natural killer cells is dramatically reduced in $irf\text{-}1^{-/-}$ mice [16]. This defect may markedly increase viral protein expression and inhibit tumor surveillance mechanisms, leading to the development of non-Hodgkin lymphoma. Expression of the IL-12 p40 subunit is defective in $irf\text{-}1^{-/-}$ mice [16].

Hypermutation of the immunoglobulin genes in B cells induced by HCV infection is the cause of the lymphomagenesis observed in HCV infection [16, 26]. This finding may provide a more direct insight into lymphoma production, because HCV-induced hypermutation causes genetic instability and chromosomal aberrations, possibly resulting in neoplastic transformation [27]. In addition, the anti-apoptotic phenotype resulting from sustained viral protein expression may enhance the survival of lymphocytes and inhibit activation-induced cell death to turn off the activated lymphocytes. The dysregulated cytokine profiles and sustained lymphocyte survival may alter the fates of regulatory T cells and dendritic cells [28].

In summary, the mouse model of B cell lymphoma and lymphoproliferative disorder represents a powerful tool to address the molecular mechanism of lymphoma development by HCV.

Conflict of Interests

The authors declare that there is no conflict of interests.

Acknowledgments

This work was supported by grants from the Ministry of Health and Welfare of Japan and the Cooperative Research Project on Clinical and Epidemiological Studies of Emerging and Re-emerging Infectious Diseases. The authors thank Drs. M. Saito, K. Kuwahara, N. Sakaguchi, M. Takeya, Y. Hiasa, S. Harada, and A. El-Gohary for their valuable collaborations.

References

[1] J. Ferlay, F. Bray, P. Pisani, and D. M. Parkin, Globocan 2000: cancer incidence, mortality and prevalence worldwide. version1.0. IARC CancerBase No. 5. IARC, Lyon, France, 2001.

[2] F. Dammacco, D. Sansonno, C. Piccoli, V. Racanelli, F. P. D'Amore, and G. Lauletta, "The lymphoid system in hepatitis C virus infection: autoimmunity, mixed cryoglobulinemia, and overt B-cell malignancy," *Seminars in Liver Disease*, vol. 20, no. 2, pp. 143–157, 2000.

[3] J. P. Gisbert, L. García-Buey, M. J. Pajares, and R. Moreno-Otero, "Prevalence of hepatitis C virus infection in B-cell non-Hodgkin's lymphoma: systematic, review and meta-analysis," *Gastroenterology*, vol. 125, no. 6, pp. 1723–1732, 2003.

[4] P. Pileri, Y. Uematsu, S. Campagnoli et al., "Binding of hepatitis C virus to CD81," *Science*, vol. 282, no. 5390, pp. 938–941, 1998.

[5] D. Rosa, G. Saletti, E. De Gregorio et al., "Activation of naïve B lymphocytes via CD81, a pathogenetic mechanism for hepatitis C virus-associated B lymphocyte disorders," *Proceedings of the National Academy of Sciences of the United States of America*, vol. 102, no. 51, pp. 18544–18549, 2005.

[6] H. Lerat, S. Rumin, F. Habersetzer et al., "In vivo tropism of hepatitis C virus genomic sequences in hematopoietic cells: influence of viral load, viral genotype, and cell phenotype," *Blood*, vol. 91, no. 10, pp. 3841–3849, 1998.

[7] S. J. Karavattathayyil, G. Kalkeri, H. J. Liu et al., "Detection of hepatitis C virus RNA sequences in B-cell non-Hodgkin lymphoma," *American Journal of Clinical Pathology*, vol. 113, no. 3, pp. 391–398, 2000.

[8] Y. Kasama, S. Sekiguchi, M. Saito et al., "Persistent expression of the full genome of hepatitis C virus in B cells induces spontaneous development of B-cell lymphomas in vivo," *Blood*, vol. 116, no. 23, pp. 4926–4933, 2010.

[9] R. C. Rickert, J. Roes, and K. Rajewsky, "B lymphocyte-specific, Cre-mediated mutagenesis in mice," *Nucleic Acids Research*, vol. 25, no. 6, pp. 1317–1318, 1997.

[10] T. Wakita, C. Taya, A. Katsume et al., "Efficient conditional transgene expression in hepatitis C virus cDNA transgenic mice mediated by the Cre/loxP system," *The Journal of Biological Chemistry*, vol. 273, no. 15, pp. 9001–9006, 1998.

[11] K. Machida, K. Tsukiyama-Kohara, E. Seike et al., "Inhibition of cytochrome c release in fas-mediated signaling pathway in transgenic mice induced to express hepatitis C viral proteins," *The Journal of Biological Chemistry*, vol. 276, no. 15, pp. 12140–12146, 2001.

[12] K. Machida, K. Tsukiyama-Kohara, S. Sekiguch et al., "Hepatitis C virus and disrupted interferon signaling promote lymphoproliferation via type II CD95 and interleukins," *Gastroenterology*, vol. 137, no. 1, pp. 285–296, 2009.

[13] K. Moriya, H. Fujie, Y. Shintani et al., "The core protein of hepatitis C virus induces hepatocellular carcinoma in transgenic mice," *Nature Medicine*, vol. 4, no. 9, pp. 1065–1067, 1998.

[14] H. Lerat, M. Honda, M. R. Beard et al., "Steatosis and liver cancer in transgenic mice expressing the structural and nonstructural proteins of hepatitis C virus," *Gastroenterology*, vol. 122, no. 2, pp. 352–365, 2002.

[15] T. Yokota, K. Oritani, I. Takahashi et al., "Adiponectin, a new member of the family of soluble defense collagens, negatively regulates the growth of myelomonocytic progenitors and the functions of macrophages," *Blood*, vol. 96, no. 5, pp. 1723–1732, 2000.

[16] S. Taki, T. Sato, K. Ogasawara et al., "Multistage regulation of Th1-type immune responses by the transcription factor IRF-1," *Immunity*, vol. 6, no. 6, pp. 673–679, 1997.

[17] D. Hockenbery, G. Nunez, C. Milliman, R. D. Schreiber, and S. J. Korsmeyer, "Bcl-2 is an inner mitochondrial membrane protein that blocks programmed cell death," *Nature*, vol. 348, no. 6299, pp. 334–336, 1990.

[18] J. C. Reed, M. Cuddy, T. Slabiak, C. M. Croce, and P. C. Nowell, "Oncogenic potential of bcl-2 demonstrated by gene transfer," *Nature*, vol. 336, no. 6196, pp. 259–261, 1988.

[19] Y. Tsujimoto, L. R. Finger, and J. Yunis, "Cloning of the chromosome breakpoint of neoplastic B cells with the t(14;18) chromosome translocation," *Science*, vol. 226, no. 4678, pp. 1097–1099, 1984.

[20] Y. Kawamura, K. Ikeda, Y. Arase et al., "Viral elimination reduces incidence of malignant lymphoma in patients with hepatitis C," *American Journal of Medicine*, vol. 120, no. 12, pp. 1034–1041, 2007.

[21] A.-R. N. Zekri, H. M. A. El-Din, A. A. Bahnassy et al., "Serum levels of soluble Fas, soluble tumor necrosis factor-receptor II, interleukin-2 receptor and interleukin-8 as early predictors of hepatocellular carcinoma in Egyptian patients with hepatitis C virus genotype-4," *Comparative Hepatology*, vol. 9, article 1, 2010.

[22] A. C. Fluckiger, P. Garrone, I. Durand, J. P. Galizzi, and J. Banchereau, "Interleukin 10 (IL-10) upregulates functional high affinity IL-2 receptors on normal and leukemic B lymphocytes," *Journal of Experimental Medicine*, vol. 178, no. 5, pp. 1473–1481, 1993.

[23] T. Taniguchi, K. Ogasawara, A. Takaoka, and N. Tanaka, "IRF family of transcription factors as regulators of host defense," *Annual Review of Immunology*, vol. 19, pp. 623–655, 2001.

[24] J. M. Penninger, C. Sirard, H.-W. Mittrücker et al., "The interferon regulatory transcription factor IRF-1 controls positive and negative selection of CD8+ thymocytes," *Immunity*, vol. 7, no. 2, pp. 243–254, 1997.

[25] M. Lohoff, D. Ferrick, H.-W. Mittrücker et al., "Interferon regulatory factor-1 is required for a T helper 1 immune response in vivo," *Immunity*, vol. 6, no. 6, pp. 681–689, 1997.

[26] K. Machida, K. T.-N. Cheng, V. M.-H. Sung et al., "Hepatitis C virus induces a mutator phenotype: enhanced mutations of immunoglobulin and protooncogenes," *Proceedings of the National Academy of Sciences of the United States of America*, vol. 101, no. 12, pp. 4262–4267, 2004.

[27] K. Machida, Y. Kondo, J. Y. Huang et al., "Hepatitis C virus (HCV)-induced immunoglobulin hypermutation reduces the affinity and neutralizing activities of antibodies against HCV envelope protein," *Journal of Virology*, vol. 82, no. 13, pp. 6711–6720, 2008.

[28] A. Dolganiuc, E. Paek, K. Kodys, J. Thomas, and G. Szabo, "Myeloid dendritic cells of patients with chronic HCV infection induce proliferation of regulatory T lymphocytes," *Gastroenterology*, vol. 135, no. 6, pp. 2119–2127, 2008.

World Journal of Vaccines, 2011, 1, 98-103
doi:10.4236/wjv.2011.13010 Published Online *** 2011 (http://www.scirp.org/journal/wjv)

Scientific Research

Evaluation of a Recombinant Measles Virus as the Expression Vector of Hepatitis C Virus Envelope Proteins

Yuri Kasama[1], Masaaki Satoh[1], Makoto Saito[1], Seiji Okada[2], Chieko Kai[3], Kyoko Tsukiyama-Kohara[1*]

[1]Department of Experimental Phylaxiology, Faculty of Life Sciences, Kumamoto University, Kumamoto, Japan; [2] Division of Hematopoiesis, Center for AIDS Research, Kumamoto University, Kumamoto, Japan; [3]Laboratory of Animal Research Center, Institute of Medical Science, University of Tokyo, Tokyo, Japan.
Email: *kkohara@kumamoto-u.ac.jp

Received June 16th, 2011; revised July 18th, 2011; accepted July 29th, 2011.

ABSTRACT

Measles virus (MV) is a negative strand RNA virus of the family Paramyxoviridae, and the attenuated Edmonston-B strain can be engineered by the reverse genetics system. Here we constructed the recombinant Edmonston strain of measles virus (MV-Ed) that expressed hepatitis C virus (HCV) envelope proteins (rMV-E1E2). The rMV-E1E2 successfully expressed HCV E1 and E2 proteins. To evaluate its immunogenicity, NOD/Scid/Jak3null mice that were engrafted with human peripheral blood mononuclear cells (huPBMC-NOJ) were infected with this rMV-E1E2. Although human lymphocytes could be isolated from the spleens of mock-infected mice during the 2-weeks-long experiment, the proportion of mice that were infected with MV or rMV-E1E2 was decreased in a viral dose-dependent manner. Over 10^3 PFU of virus infection decreased the human PBL to less than 5%. Significant decrease of B cell population in human PBL from rMV-E1E2 infected NOD-SCID mice and decrease of T cell population in those from MV infected mice were observed. Human antibody production in these mice was also examined. Thus, the results in this study may contribute for future improvement of recombinant vaccine using measles virus vector.

Keywords: *MV, HCV, E1, E2, Human PBMC, NOD/Scid/Jak3null Mouse*

1. Introduction

Measles virus (MV) is classified into the family *Paramyxoviridae*. Its genome is composed of 15,894 nucleotides, which encodes a nucleocapside protein (N), phospho protein (P), matrix (M), haemaglutinin (H), fusion (F), and viral polymerase (L). The establishment of the reverse genetic system for the rescue of an attenuated Edmonston-B stain from cloned DNA [1] enabled to develop measles virus as virus expression vector. Subsequently, a number of foreign proteins have been efficiently expressed. Efforts to develop vaccines using recombinant MV expressing different proteins derived from dengue virus [2,3], human immunodeficiency virus [4], HPV[5], SARS [6], or West Nile virus [7] have been reported.

The MV vaccine is a well-known, live-attenuated vaccine and has proven to be one of the safest, most stable, and effective human vaccines [8]. This vaccine is produced on a large scale in many countries and used at low cost through the Extended Program on Immunisation of the WHO [9,10]. While this vaccine has been shown to induce life-long immunity with a single dose, boosting is effective. Thus, MV possesses a high potential for the vaccine vector.

Hepatitis C virus (HCV) is a member of the *Flaviviridae* family and is the causative agent of both chronic hepatitis and hepatocellular carcinoma (HCC) [11]. 170 million people are infected with HCV worldwide [12,13]. Despite prevention efforts and advanced treatment strategies, including combined PEGylated IFN-α and ribavirin therapy [14,15], the clinical efficacy of this treatment is limited [16,17]. Alternative novel antiviral agents that have been shown to elicit effective responses in chronically infected patients, such as inhibitors of viral protease, helicase, and polymerase, are currently being developed but are expensive [18]. Therefore, the development of an effective vaccine is important.

Immunological approaches to control HCV infection

Copyright © 2011 SciRes.

have proven to be ineffective, in part because HCV adapts to escape from the host immune system [19]. Furthermore, a high percentage of immunocompetent individuals are infected by HCV despite their ability to mount an active immune response [20]. A preventive HCV vaccine is required to protect unexposed individuals from HCV infection. This vaccine will most likely need to target the viral envelope glycoproteins, E1 and E2.

HCV research has long been hampered by the lack of an animal model that reproduces HCV infection in humans. The model in which severe combined immunodeficient (SCID) mice are transplanted with human peripheral blood mononuclear cells (PBMC) is a well-established system to study human immunity (hu-PBMC-SCID). This mouse develops all human lymphoid cell lineages that repopulate the animal's lymphoid organs. Our group previously generated the non-obese diabetic (NOD)/SCID/Janus kinase 3 (Jak3) knockout (NOJ) mouse model and then established a human hemolymphoid system in this mouse [21,22]. In this study, we infect human PBMC-transplanted NOJ mice with MV and rMV-E1E2 and then characterise their infectivity and effects in the transplanted human cells.

2. Materials and Method

2.1. Cells

B95a cells, a marmoset B cell line[23], were used for viral titration and rescue, and were maintained in RPMI 1640 medium supplemented with 10% heat-inactivated foetal calf serum (FCS).

2.2. Plasmid Construction and Viral Rescue

The cDNAs encoding HCV E1 and E2 were obtained from the plasmid HCR6CNS2 [24]. We used replication-competent MV-based vectors (pMV; MV Edmonston strain) [1]. The E1 and E2 cDNAs were cloned into the *Fse* I site of pMV and the resulting clone, pMV-E1E2, was used to rescue the infectious recombinant MV expressing the HCV envelope glycoproteins (rMV-E1E2), as reported previously [25,26].

2.3. Generation of Humanised Mice

Mice were reconstituted as described previously [21,22]. The NOD/SCID/JAK3^{null} strain was established by backcrossing JAK3^{null} and the NOD Cg-Prkdc^{Scid} strains for ten generations. All animal experiments were performed according to the guidelines of Institutional Animal Committee or Ethics Committee of Kumamoto University.

2.4. Preparation of Human Blood Leukocytes and Transplantation

Peripheral blood mononuclear cells were isolated from blood donors using Ficoll-Hypaque density gradient centrifugation. A total of 5×10^6 cells were transplanted into the spleen of irradiated (2 Gy) 4-weeks-old mice.

2.5. MV and rMV-E1E2 Infection

We injected 100 - 104 PFU of MV or 100 - 102 or 104 PFU of rMV-E1E2 intraperitoneally for MV and rMV-E1E2 infection, respectively. As a negative control, a group of mice was injected with RPMI 1640. Mice were moni- tored for 2 weeks and then euthanised. The spleens and peripheral blood were collected for analysis.

2.6. Flow Cytometry

Isolated splenocytes were stained with APC-Cy7-conjugated anti-mouse CD45 (BD Pharmin-gen) to detect the murine lymphocytes and either APC—or pacific blue-conjugated anti-human CD45 (DAKO), hCD3-PE/Cy7, hCD19-FITC, hCD4-PE, and hCD8-PB (BD Biosciences) to detect human lymphocytes. All data were analysed using FlowJo (Tree Star).

2.7. Confirmation of Viral Infection

The viral infection of the human lymphocytes was con-firmed using co-culture with B95a cells followed by RT-PCR. Suspensions of isolated splenocytes were co-cultured with B95a cells and the formation of cytopathic effects (CPEs) was monitored for 2 weeks. Additionally, RNA was isolated from the supernatant of the co-cultures using ISOGEN-LS (Nippon gene) according to manufacturer's instructions. MV RNA was detected using RT -PCR with the sense primer, 5'-ACTCGGTATCACTGCCGAGGATGCAAGGC-3' (1256 - 1284) and antisense primer 5'-CAGCGTCGTCATCGCTCTCTCC-3'(2077 - 2056) or 5'-ATGGCAGAAGAGCAGGCACG-3'(1807 - 1826). HCV E1 or E2 was amplified using E1-S-1051 5'-CCGTTGCTGGGTGGCACTTA-3 and E1-AS-1314 5'-ATCATCATGTCCCAAGCCAT-3' or E2-S-1600 5'-CTGGCACATCAACAGGACTG-3' and E2-AS-1960 5'-AAGGAGCAGCACGTCTGTCT-3'.

2.8. ELISA

Anti-MV antibody titers were determined by using an ELISA assay. 96-well plates were coated with a 25 g/ml solution of MV-infected B95a lysate or recombinant E2-expressing baculovirus-infected Sf9 lysate as antigen, respectively. The plates were consecutively incubated with sera (1:100) recovered from hu-PBL-NOJ mice, peroxidase-conjugated rabbit-human IgG (DAKO), and TMB Peroxidase EIA Substrate Kit (Bio-Rad) at 37°C for 1 h. Optical density values were measured at 450 nm.

2.9. Western Blot Analysis

Total protein extracts from E2-expressing baculovirus-in-

Copyright © 2011 SciRes.

fected Sf9 lysate were separated by SDS-PAGE. The primary antibodies used for western blots were as follows: sera from mice (1:100) and anti-E2 monoclonal antibody (1:5000). Peroxidase-conjugated secondary antibodies were added and incubated with the mixture for 1 h at room temperature. Bound antibody was visualized using ECL reagent (Amersham Bioscience) with LAS1000 scanner (Fuji film).

3. Results

3.1. Construction of Recombinant Measles Virus Expressing HCV E1 and E2 Proteins

The HCV genes corresponding to the envelope proteins E1 and E2 were sub-cloned in between the N and P genes of the MV vector (**Figure 1(a)**). The HCV E1 and E2 genes included the putative signal peptide sequences at the N terminus and the transmembrane domain at the C terminus [27]. The plasmid vector pMV-E1E2 was introduced with supporting plasmids into 293T cells to rescue the recombinant viruses. The expression of the HCV E1 and E2 proteins by rMV-E1E2 was examined by western blotting (**Figure 1(b)**).

3.2. Infection of hu-PBMC-NOJ Mice with MV and rMV-E1E2

All hu-PBMC-NOJ mouse infections were 14 days long. Infections with MV and rMV-E1E2 were confirmed by first co-culturing the human lymphocytes isolated from the spleens of infected mice with B95a cells and then verifying the presence of virus by RT-PCR. In all the MV (10^3 - 10^4 PFU) or rMV-E1E2 (10^4 PFU)-infected hu-PBMC-NOJ mice, CPEs were observed in co-cultures containing splenocytes that were isolated from infected mice (**Table 1**). The results of the co-culture assays are in agreement with results that were obtained by RT-PCR; positive bands were observed in the mice infected with 10^3 - 10^4 PFU of MV and 10^2, 10^4 PFU of rMV-E1E2 (**Table 1**). These results demonstrate that the rescued MV and rMV-E1E2 are able to infect transplanted human PBMCs.

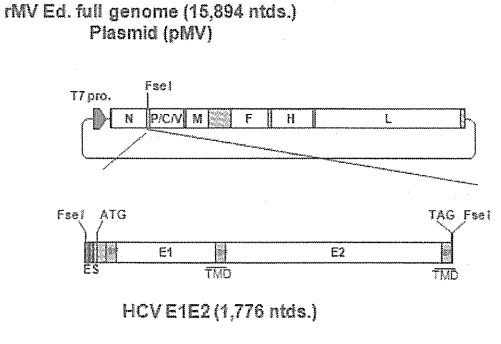

(a)

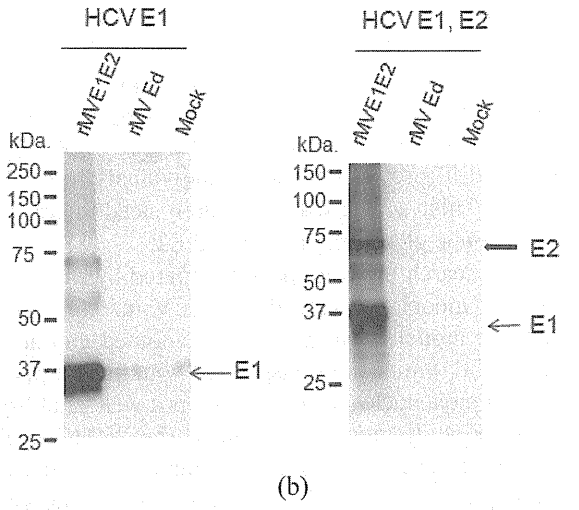

(b)

Figure 1. Construction of the recombinant MV vectors. (a) The rMV full genome vector derived from the MV-Ed strain is illustrated in the upper panel and is labelled with letters as follows: N, nucleocapsid; P, phosphoprotein; M, matrix; F, fusion; H, hemagglutinin; and L, large. T7 indicates the T7 RNA polymerase promoter. The cDNA encoding the HCV envelope glycoproteins (E1 and E2) containing the signal peptide sequence (SP) and the transmembrane domain (TMD, underlined) regions, the N gene end signal (E), the P gene start signal (S), and the intercistronic region of the H protein genes at the 5' end, which was flanked by Fse I sites at both ends, was introduced into the unique Fse I site in between the N and P genes in the pMV vector. The resulting plasmid was designated pMV-E1E2. (b) The HCV E1 and E2 proteins were detected in rMV-E1E2-, rMV-Ed- and mock-infected B95a cells by western blot with MoAb 384 for E1 and MoAb 384 and 544 for E1 and E2 (arrows).

3.3. Proportion of Engrafted Human Lymphocytes in MV- and rMV-E1E2- Infected Hu-PBMC-NOJ Mice

The splenocytes that were isolated from infected mice were analysed using flow cytometry to determine the proportion of human cells in the spleen (**Table 1**, **Figure 2**). In the MV-infected hu-PBMC-NOJ mice, a population of human lymphocytes was observed in the mice that were infected with 10^0 - 10^2 PFU, whereas few human lymphocytes were observed in mice infected with 10^3 - 10^5 PFU. In the rMV-E1E2-infected mice, a population of human lymphocytes was detected in mice that were inoculated with 10^0 - 10^2 PFU. The ratio of human lymphocyte settlement in both groups of mice was inversely correlated with the results from the RT-PCR and co-culture assays (**Table 1**). The B cell population of rMV-E1E2 infected human lymphocytes was significantly decreased than medium control (**Figure 2**). In contrast, the

Copyright © 2011 SciRes.

Table 1. Summary of MV infection to human PBL in NOD/Scid mice.

Virus	Amount of virus	No. tested	huPBL settlement (Av.+/−SD%)	CPE*	Viral RNA**	ELISA[@] MV	ELISA[@] E2
Mock	0	6	90.9 ± 13.1	0/6	0/6	ND[#]	ND
MV	10^0	3	92.7 ± 11.2	0/3	0/3	1/3	ND
	10^1	3	58.4 ± 50.6	0/3	0/3	2/3	ND
	10^2	3	55.1 ± 49.9	0/3	0/3	ND	ND
	10^3	2	4.9 ± 6	2/2	2/2	ND	ND
	10^4	2	1.7	2/2	2/2	ND	ND
	10^5	2	3.7	NT[+]	NT	ND	ND
MV-E1E2	10^0	2	79.6	0/2	0/2	ND	ND
	10^1	2	96.0	0/2	0/2	2/2	ND
	10^2	3	56.2 ± 36.2	0/3	1/3	1/3	1/3
	10^4	4	0.34 ± 0.004	4/4	4/4	ND	ND

*CPE formation in B95a cells co-cultured with PBL from each mice; **Detection of MV or HCV-RNA in PBL by RT-PCR. +NT; not tested; [#]Not detected. [@]Human antibody was detected by ELISA.

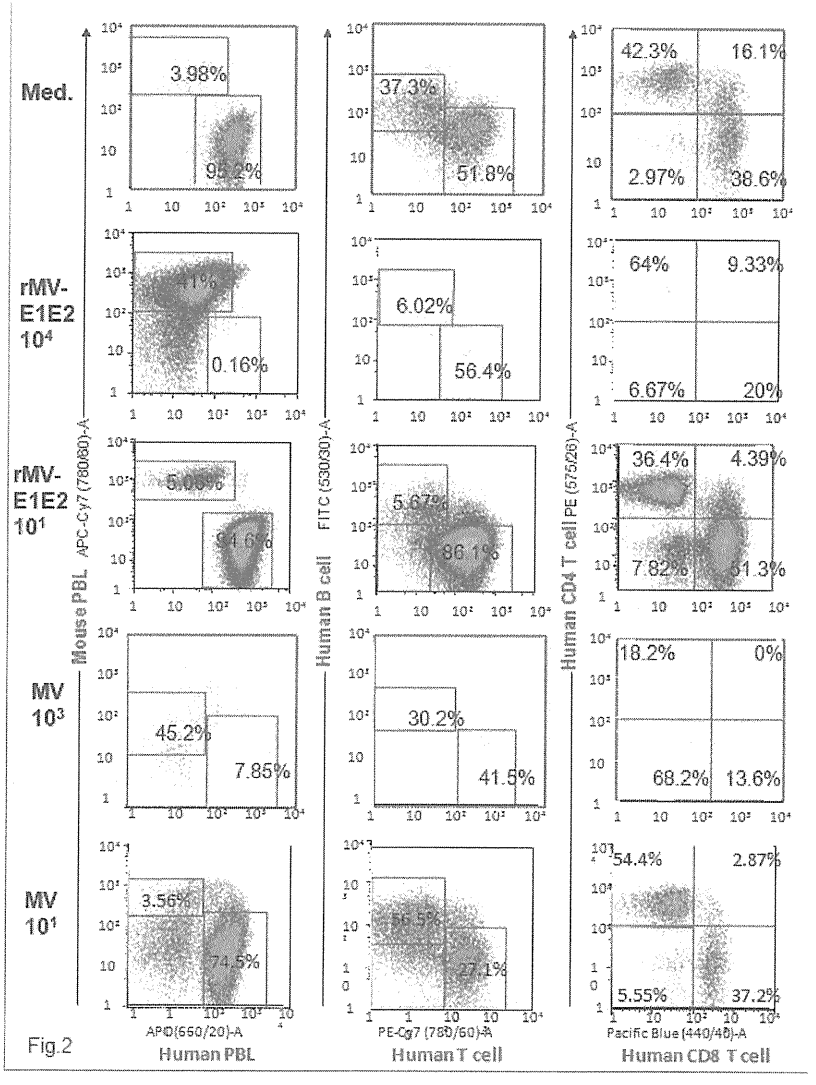

Figure 2. Flow cytometric analysis of splenocytes isolated from hu-PBMC-NOJ mice inoculated with medium, rMV-E1E2 (10^1, 10^4 PFU), or MV-Ed (10^1, 10^3 PFU). Splenocytes, consisting of both human and murine cells, were stained with antibodies against human or mouse CD45. Human PBL was further stained with hCD3-PE/Cy7, hCD19-FITC, hCD4-PE, and hCD8-PB. Representative flow cytometric profiles of each group of infected mice are shown. The percentage of lymphocytes are shown by numbers.

Copyright © 2011 SciRes.

T cell population of MV infected human lymphocytes were significantly decreased than medium control.

To examine the immune response against MV and rMV-E1E2 by the transplanted human PBMCs, we measured human MV- or HCV-specific antibodies using an ELISA with an MV-infected B95a cell lysate or recombinant HCV E2 protein. A significant amount of human antibody against MV antigens was detected in the sera from mice that were infected with MV (10^0 PFU 1/3, 10^1 PFU 2/3) or rMV-E1E2 (10^1 2/2, 10^2 PFU 1/3). However, only one mouse, which was infected with 10^2 PFU of rMV-E1E2, generated human antibodies against HCV E2 (10^2 PFU 1/3), which was confirmed by western blot analysis (**Table 1**).

4. Discussion

The results in this study revealed that more than 10^3 PFU of MV or 10^4 PFU of rMV-E1E2 infection decreased the human PBL to less than 5%. We detected a significant amount of MV-specific antibodies in the rMV-E1E2-infected mice (n = 3). However, only one mouse produced E2-specific antibodies and no mice produced E1-specific antibodies. These results may be consistent with the hypothesis that the immunogenicity of the E1 and E2 proteins might be lower than the immunogenicity of the MV proteins, an observation that is consistent with previous studies [28-31]. Future studies are required to clarify the immune response to HCV envelope proteins and protection of viral infection.

In summary, we infected human PBMC–transplanted NOJ mice with MV and rMV-E1E2 and then characterised the humoral immune responses elicited by the transplanted human cells. The results in this study revealed the possibility and improvement of rMV-E1E2 and the potential and the limit of hu-PBMC-NOJ mice for the evaluation of the immunogenicity of viral proteins.

Further development of the rMV-E1E2 and hu-PBMC - NOJ mouse model system will allow us to develop potential vaccine targets, which are indispensable for the development of an effective vaccine.

5. Acknowledgements

We would like to thank M. A. Billeter and K. Takeuchi for providing the MV Edmonston B strain rescue system, S. Iwanaga, K. Tanaka, F. Ikeda and M. Yoneda for their technical support, and M. Kohara for providing the anti-E1 and E2 antibodies. This work was supported by grants from the Ministry of Health and Welfare of Japan, and the Ministry of Education, Culture, Sports, Science and Technology of Japan.

REFERENCES

[1] F. Radecke, P. Spielhofer, H. Schneider, *et al.*, "Rescue of Measles Viruses from Cloned DNA," *EMBO Journal*, Vol. 14, No. 23, 1995, pp. 5773-5784.

[2] S. Brandler, M. Lucas-Hourani, A. Moris, *et al.*, "Pediatric Measles Vaccine Expressing a Dengue Antigen Induces Durable Serotype-Specific Neutralizing Antibodies to Dengue Virus," *PLoS Neglected Tropical Diseases*, Vol. 1, No. 3, 2007, pp. e96-e108. doi:10.1371/journal.pntd.0000096

[3] S. Brandler and F. Tangy, "Recombinant Vector Derived from Live Attenuated Measles Virus: Potential for Flavivirus Vaccines," *Comparative Immunology, Microbiology and Infectious Diseases*, Vol. 31, No. 2-3, 2008, pp. 271-291. doi:10.1016/j.cimid.2007.07.012

[4] C. Lorin, L. Mollet, F. Delebecque, *et al.*, "A Single Injection of Recombinant Measles Virus Vaccines Expressing Human Immunodeficiency Virus (HIV) Type 1 Clade B Envelope Glycoproteins Induces Neutralizing Antibodies and Cellular Immune Responses to HIV," *Journal of Virology*, Vol. 78, No. 1, 2004, pp. 146-157. doi:10.1128/JVI.78.1.146-157.2004

[5] G. Cantarella, M. Liniger, A. Zuniga, *et al.*, "Recombinant Measles Virus-HPV Vaccine Candidates for Prevention of Cervical Carcinoma," *Vaccine*, Vol. 27, 2009, pp. 3385-3390. doi:10.1016/j.vaccine.2009.01.061

[6] M. Liniger, A. Zuniga, A. Tamin, *et al.*, "Induction of Neutralising Antibodies and Cellular Immune Responses against SARS Coronavirus by Recombinant Measles Viruses," *Vaccine*, Vol. 26, No. 17, 2008, pp. 2164-2174.

[7] P. Despres, C. Combredet, M. P. Frenkiel, *et al.*, "Live Measles Vaccine Expressing the Secreted Form of the West Nile Virus Envelope Glycoprotein Protects against West Nile Virus Encephalitis," *Journal of Infectious Diseases*, Vol. 191, No. 2, 2005, pp. 207-214. doi:10.1086/426824

[8] C. Combredet, V. Labrousse, L. Mollet, *et al.*, "A Molecularly Cloned Schwarz Strain of Measles Virus Vaccine Induces Strong Immune Responses in Macaques and Transgenic Mice," *Journal of Virology*, Vol. 77, No. 21, 2003, pp. 11546-11554. doi:10.1128/JVI.77.21.11546-11554.2003

[9] D. Naniche, M. Garenne, C. Rae, *et al.*, "Decrease in Measles Virus-Specific CD4 T Cell Memory in Vaccinated Subjects," *Journal of Infectious Diseases*, Vol. 190, 2004, pp. 1387-1395. doi:10.1086/424571

[10] I. G. Ovsyannikova, N. Dhiman, R. M. Jacobson, R. A. Vierkant and G. A. Poland, "Frequency of Measles Virus-Specific CD4+ And CD8+ T Cells in Subjects Seronegative or Highly Seropositive for Measles Vaccine," *Clinical and Diagnostic Laboratory Immunology*, Vol. 10, No. 3, 2003, pp. 411-416.

[11] A. M. Di Bisceglie, R. L. Carithers Jr. and G. J. Gores, "Hepatocellular Carcinoma," *Hepatology*, Vol. 28, No. 5, 1998, pp. 1161-1165. doi:10.1002/hep.510280436

[12] Global Surveillance and Control of Hepatitis C, "Report of a WHO Consultation Organized in Collaboration with the Viral Hepatitis Prevention Board, Antwerp," *Journal of Viral Hepatitis*, Vol. 6, No. 1, 1999, pp. 35-47.

Copyright © 2011 SciRes.